Journal of African Earth Sciences 130 (2017) 293–318

Contents lists available at ScienceDirect

Journal of African Earth Sciences

journal homepage: www.elsevier.com/locate/jafrearsci

Sedimentology of the Essaouira Basin (Meskala Field) in context of regional sediment distribution patterns during upper Triassic pluvial events

Nadine K. Mader [a, *], Jonathan Redfern [a], Majid El Ouataoui [b]

[a] North Africa Research Group, School of Earth, Atmospheric and Environmental Sciences, University of Manchester, Williamson Building, Oxford Road, Manchester, M13 9 PL, United Kingdom
[b] ONHYM, 5 Avenue Moulay Hassan, B.P.99, 10050, Rabat, Morocco

ARTICLE INFO

Article history:
Received 23 March 2016
Received in revised form
19 December 2016
Accepted 6 February 2017
Available online 8 February 2017

Keywords:
Upper Triassic
Morocco
Depositional reservoir model
Regional sediment distribution
Triassic climate

ABSTRACT

Upper Triassic continental clastics (*TAGI: Trias Argilo-Greseux Inferieur*) in the Essaouira Basin are largely restricted to the subsurface, which has limited analysis of the depositional environments and led to speculation on potential provenance of the fluvial systems. Facies analysis of core from the Meskala Field onshore Essaouira Basin is compared with tentatively time-equivalent deposits exposed in extensive outcrops in the Argana Valley, to propose a process orientated model for local versus regional sediment distribution patterns in the continuously evolving Moroccan Atlantic rift during Carnian to Norian times. The study aims to unravel the climatic overprint and improve the understanding of paleo-climatic variations along the Moroccan Atlantic margin to previously recognised Upper Triassic pluvial events.

In the Essaouira Basin, four facies associations representing a progressive evolution from proximal to distal facies belts in a continental rift were established. Early ephemeral braided river systems are succeeded by a wet aeolian sandflat environment with a strong arid climatic overprint (FA1). This is followed by the onset of perennial fluvial deposits with extensive floodplain fines (FA2), accompanied by a distinct shift in fluvial style, suggesting increase in discharge and related humidity, either locally or in the catchment area. The fluvial facies transitions to a shallow lacustrine or playa lake delta environment (FA3), which exhibits cyclical abandonment. The delta is progressively overlain by a terminal playa with extensive, mottled mudstones (FA4), interpreted to present a return from cyclical humid-arid conditions to prevailing aridity in the basin.

In terms of regional distribution and sediment source provenance, paleocurrent data from Carnian to Norian deposits (T5 to T8 member) in the Argana Valley suggest paleoflow focused towards the S and SW, not directed towards the Meskala area in the NW as previously suggested. A major depo-centre for fluvial sediments is instead located in the southern Argana Valley, possibly the Souss Basin. To effectively source the reservoir sandstones found in the Meskala Field, a more local provenance area has hence to be envisaged. Despite this, the direct comparison of the genetic evolution of sedimentary sequences in the Argana Valley and Essaouira Basin shows a similar progression from dominantly arid ephemeral depositional environments to humid perennial sedimentation, returning to prominent arid conditions. This suggests climatic control in both regions, where an enhanced humid signal drives perennial fluvial flow in otherwise arid dominated sequences. On a regional scale, this is suggested to record the impact of strong Triassic pluvial events previously recognised in other basins along the Central Atlantic margin during the Carnian to Norian periods.

1. Introduction

Prior to the exploration efforts in SW Morocco, the development of new theories about global continent evolution during the initial stages of rifting along the Atlantic margin had already highlighted

* Corresponding author. Current Address: Maersk Oil Norge AS, Moseidsletta 122, 4068 Stavanger, Norway.
E-mail address: madernadine@hotmail.com (J. Redfern).

http://dx.doi.org/10.1016/j.jafrearsci.2017.02.012
1464-343X/

the importance of the investigated Moroccan basins for global pre-drift reconstructions (e.g. Van Houten, 1977; Manspeizer et al., 1978; Jansa and Wiedmann, 1980; Stets and Wurster, 1981; Hinz et al., 1981; Manspeizer, 1982, 1988; Laville and Petit, 1984; Beauchamp, 1988; Medina, 1991, 1995; Piqué and Laville, 1996; Piqué et al., 1998; Baudon et al., 2012; Leleu et al., 2016). With the discovery of hydrocarbons in the central part of the Agadir-Essaouira Basin (Fig. 1) in the early 1990's numerous studies evaluated the Triassic petroleum systems of Morocco (e.g. Broughton and Trépanier, 1993; Morabet et al., 1998; Hafid et al., 2000; Bouatmani et al., 2004). Apart from a facies classification based on electrical log character of wells in the Meskala Field (Bouatmani et al., 2004), most studies have a strong focus on the structural evolution, with little focus on integrated sedimentological analysis, leaving the regional facies distribution and provenance for the prolific Upper Triassic sandstone reservoirs within the greater Agadir-Essaouira Basin open to speculation. Broughton and Trépanier (1993) for example suggested the entire Triassic sequence of the Argana Valley as the eastward extension of the central Essaouira Basin, hence part of the sediment routing from the provenance area, while seismic interpretations and new dating of the overlying basalts led Hafid et al. (2000) to the conclusion, that only the upper part (Middle to Upper Triassic) of the Argana series was connected to the central Essaouira Basin, whereas the lower part was deposited in an isolated rift arm.

To-date, the relationship between Upper Triassic clastic sediments in the Argana Valley to Triassic reservoir sandstones of the central Essaouira Basin remains uncertain. In order to improve the regional understanding of the spatial distribution of these extensive fluvio-aeolian reservoir facies in SW Morocco, this study presents new sedimentological analyses of core data from the central Essaouira Basin (Meskala Field), integrated with results from sedimentological outcrop studies of the Argana Valley (Tadrart Ouadou Sandstone member, T6; Mader, 2005; Mader and Redfern, 2011), and additional published descriptions for Carnian-Norian deposits from the Argana Valley exposures (Brown, 1980; Hofmann et al., 2000). The study aims to integrate the sedimentological data within a regional climatic framework, improving the understanding of the control on sedimentation of extreme Triassic humid events as summarised by Preto et al. (2010) or proposed by Arche and Lopez-Gomez (2014) for example.

2. Geological setting

Triassic sediments in Morocco outcrop within the Middle and High Atlas mountain chain, along the western margin of the African platform, and have also been encountered by wells in the Essaouira and Souss Basins, and along the present offshore Moroccan continental margin (Fig. 1). The Triassic sequences of Northwest Africa typically overlay a major unconformity and are deposited on Palaeozoic rocks deformed by the Hercynian and older orogenies. Deposition of the Triassic sequences took place in a series of (half-) grabens or strike-slip basins related to rifting along the Atlantic margin during the break-up of the Pangaean continent (Mattis, 1977; Van Houten, 1977; Manspeizer et al., 1978; Laville and Petit, 1984; Medina, 1988, 1991, 1995) (Figs. 1 and 2). Recent research suggests a change in how rift-basin geometry along the Central Atlantic Margin is viewed, and rather than the typical narrow rift-basin geometries more uncharacteristic broad sag-type basin styles have been reported, particularly for the Eastern provinces (Baudon et al., 2012; Leleu et al., 2016). The Triassic deposits infilling these basins commonly consist of coarse alluvial conglomerates, continental fluvial or aeolian sandstones, and alternations of fine siltstones, with evaporitic or non-evaporitic (playa) mudstones. In most parts of Morocco, the Triassic red beds are capped by the CAMP basalts (Central Atlantic Margin Province), which in turn are conformably transgressed, or interfinger, with limestones, dolomites, algal stromatolites, anhydrites, mudstones and halite deposits of an Early Jurassic sabkha environment (e.g. Courel et al., 2003).

3. Structural evolution

Mesozoic sequences in SW Morocco record the break-up of the super-continent Pangaea where crustal thinning and deep seated thermal activity led to the development of the Atlantic Ocean (Veevers, 1994). The Moroccan passive margin on the eastern side of the central Atlantic Ocean (e. g. Van Houten, 1977; Manspeizer et al., 1978; Piqué et al., 1998) demonstrates at least four major tectonic phases influencing deposition of Latest Palaeozoic to Early Mesozoic strata (Manspeizer et al., 1978; Laville and Petit, 1984; Piqué et al., 1998). In a time period covering the Permian to the Middle Triassic, extensive uplift with related crustal thinning along the axis of the future Atlantic defines the initial phase of break-up (Van Houten, 1977). The second, late Middle Triassic tectonic phase, resulted in strike-slip faulting along E-trending fracture zones and initiated W trending Tethys transgressions (Piqué et al., 1998). During the Late Triassic, continued rifting along the proto-Atlantic axis led to the deposition of clastic-evaporite sequences up to 5000 m thick in a relatively broad rift-setting with sag-geometries (Leleu et al., 2016) (Figs. 1 and 2B). Shearing occurred dominantly along E- to W-trending fracture zones inducing the decoupling of African and North American segments (Manspeizer et al., 1978), creating a pathway for Tethyan transgressions from E to W. In a last major tectonic phase (Late Triassic to Early Jurassic) global plate reorganisation led to crustal extension and seafloor spreading, resulting in massive extrusions of olivine and quartz tholeiitic basalts and igneous rock emplacement across a large area of North America and West Africa described as the Central Atlantic Margin Province (CAMP) (Marzoli et al., 1999; McHone, 2000; Olsen et al., 2000; Youbi et al., 2003; Knight et al., 2004; Marzoli et al., 2004; Verati et al., 2007; Whiteside et al., 2010; Deenen et al., 2010). During this last phase, a strong transcurrent component with transtension is proposed by Laville and Petit (1984), while Piqué et al. (1998) suggest normal faulting during this final syn-rift stage in Morocco.

4. Basin fill

The Agadir-Essaouira Basin forms part of the El Jadida-Agadir rift segment (Fig. 1). It developed as a set of half-grabens and underlies an extensive area of the modern day eastern passive Atlantic margin (Piqué et al., 1998). The nomenclature utilised to describe the Agadir-Essaouira Basin varies widely due to the complex basin segmentation and the lack of sufficient sub-surface or outcrop control (e.g. Société Chérifienne des Pétroles, 1966; Brown, 1980; Broughton and Trépanier, 1993; Piqué et al., 1998; Hafid, 2000). For consistency, the sediments of the Meskala Field are described in this paper as clastics deposited within the “central Essaouira Basin”, and the term “Argana Valley” is adopted synonymously to describe clastic deposits exposed in the present day Argana physiographic depression due to the lack of a so far clearly defined outline or structural framework for a potential “Argana Basin”.

4.1. Central Essaouira Basin (Meskala Field)

The Essaouira Basin is situated in central western Morocco and extends towards the N and S of the city of Essaouira, offshore and onshore, along the present day coastline (Figs. 1 and 2). The central basin is limited in the N by the Tensift-fault zone, and to the S by the

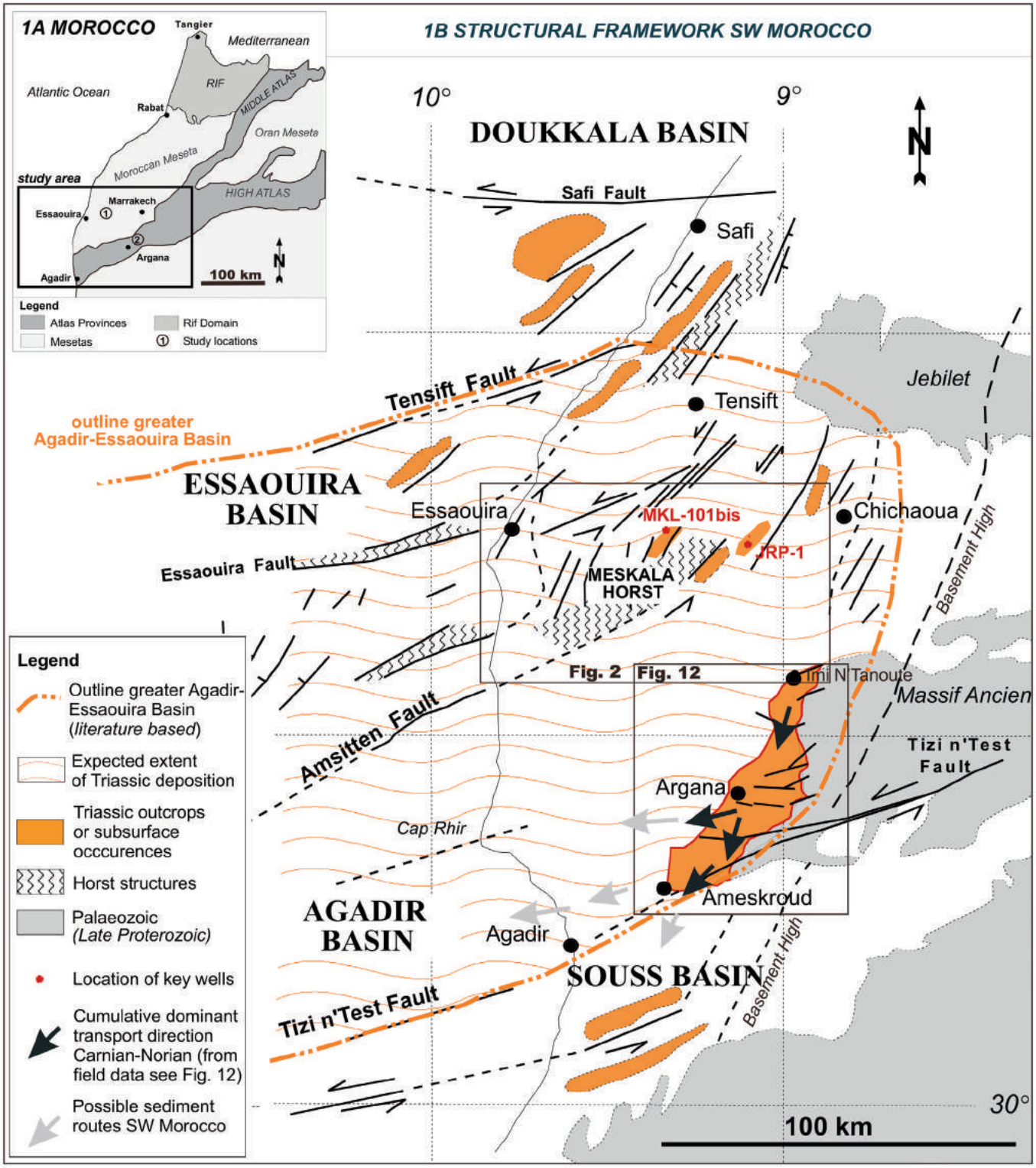

Fig. 1. A (inset) Location map of Morocco displaying the main structural domains with the WSW-ENE trending High Atlas, the SW-NE trending Middle Atlas, the Rif domain in the North, and the Moroccan and Oran Mesetas located in central Western and Eastern Morocco. The subsurface study was carried out in the central Essaouira Basin (1) on core of wells from the Meskala Field, while the outcrop study was undertaken in the Argana Valley (2), exposing extensive Permo-Triassic strata along the southern extends of the High Atlas mountain chain. **B** The map displays the structural framework of Mesozoic (Triassic to Early Jurassic) basins in SW Morocco (modified after LeRoy and Piqué (2001); with additions for the Argana Valley modified after Brown, 1980). Triassic depo-centres either known from outcrop or the sub-surface are marked in orange, and key wells are marked in red (e.g. well MKL101*bis*). In the literature several of the SW-NE to WSW-ENE trending sub-basins and half-grabens displayed are summarised as the Agadir-Essaouira Basin (orange dotted line). For the Argana Valley paleocurrent data for Carnian to Norian deposits (compilation from Brown, 1980; Mader, 2005; Mader and Redfern, 2011) are superimposed on the structural map of SW Morocco: black arrows are supported by field data, whereas grey arrows mark anticipated transport routes. Within the Argana Valley exposures, field data suggests main transport direction towards the S, SW locally to the W (see Fig. 12 for more detail). Only minor fluvial deposits show clear SE to NW flow directions, which could indicate a direct sediment transport link to the Meskala field. (For interpretation of the references to colour in this figure legend, the reader is referred to the web version of this article.)

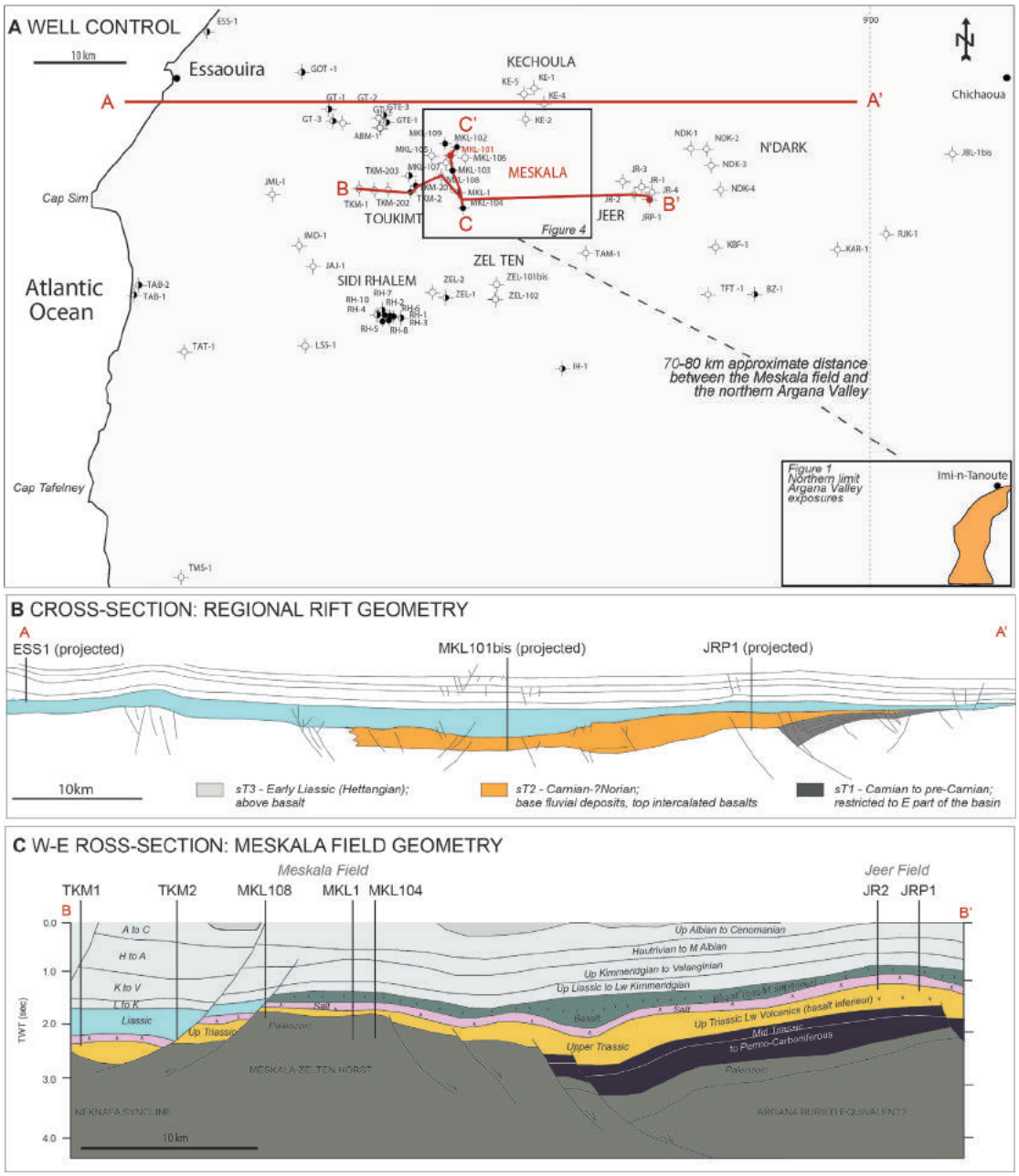

Fig. 2. **A** shows the surface locations of key wells in the greater onshore Essaouira Basin as well as the approximate location and distance to the outcrop exposures in the Argana Valley to the SE (orange). The Meskala Field lies in the central part of the explored Essaouira Basin, and the red lines mark key cross-sections that are displayed and discussed in Figs. 2B,C, 4. **B** The W-E running cross-section (A-A′) exhibits the subsurface distribution of Triassic to Early Jurassic major depositional sequences. An overall broad rift-basin morphology with a west-ward shift of main depositional units is apparent, and Carnian to Norian sandstones (sT2) extend across the prominent Meskala-Zelten horst (see also Fig. 2C) (simplified cross-section is based on seismic interpretations by Piqué et al. (1998) and LeRoy and Piqué (2001)). **C** The close-up integrated well and seismic correlation (B-B′) across the Meskala Field into the Jeer Field to the E shows clear thinning of Upper Triassic reservoir units across the horst towards the W (modified after Broughton and Trepanier, 1993). Along the top, the Upper Triassic is bound by salt deposits and an extrusive basalts (*basalt superieur*) capping the reservoir units sub-regionally. The basalt is subsequently overlain by Early Jurassic deposits and younger sedimentary units (see also **2B;** sT3). In the E part towards the Jeer Field, sills can be intrusive into the Upper Triassic deposits (*basalt inferieur*). The key well discussed in this study Mkl101*bis* is located in a central to northern position of the Meskala Field (**2A**). Offset wells MKL1 and MKL4 (**2A,C**) contain Ostracodes (*Darwinula, Lymnocythere)* (Silmane and ElMostaine, 1997), suggesting a Carnian to Norian age for the investigated Triassic deposits. Absolute ages for intrusive dolerites from adjacent well JRP-1 (**2A,C**) yield a Norian age (210 Ma). (For interpretation of the references to colour in this figure legend, the reader is referred to the web version of this article.)

Amsitten fault complex (Fig. 1). The basin contains an up to 4500 m thick sequence of Mesozoic strata (Broughton and Trépanier, 1993) (Fig. 3). Middle Triassic to Lower Jurassic continental red beds were deposited in an extensional rift setting, overlain by several kilometres of salt (Fig. 2C). Salt deposition was largely driven by marine incursions into the deepening basins from the Tethys during Upper Triassic to Lower Jurassic times (Courel et al., 2003). Extensive emplacement of basalts reaching thicknesses of up to several hundred meters occurred around the Triassic-Jurassic boundary, and can be related to the CAMP magmatism (McHone, 2000; Knight et al., 2004; Nomade et al., 2007; Deenen et al., 2010) (Fig. 2C). During the Atlasic (Alpine) tectonic phase from Late Eocene to

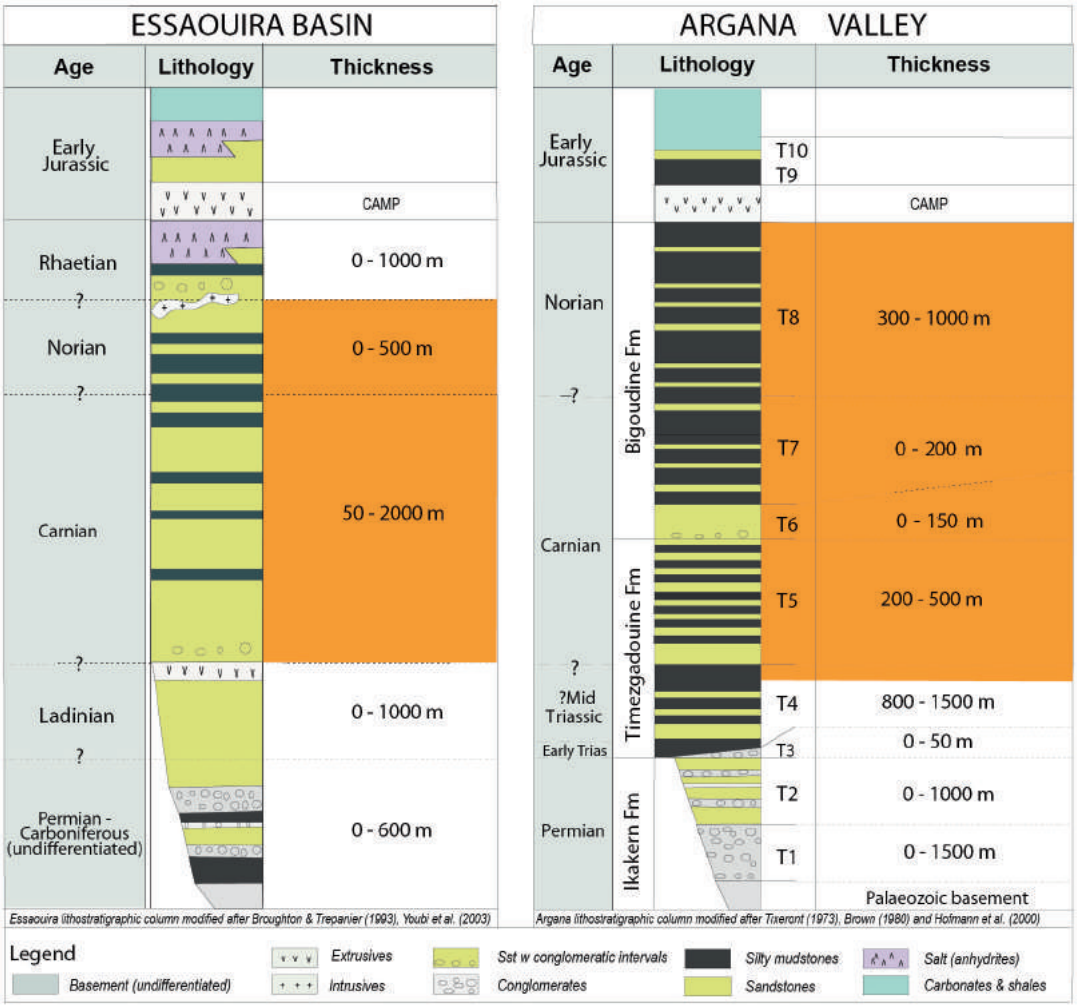

Fig. 3. Stratigraphic columns of the Essaouira Basin (left) and the Argana sequence (right), summarising major lithostratigraphic units for both study areas. For the Argana sequences lithostratigraphic members (T1-T10) and corresponding formations are displayed (after Tixeront, 1973; Brown, 1980). Members T5-T8 represent deposits of Carnian to Norian age that are considered to represent the time equivalent sequences in the Meskala Field in Essaouira (both highlighted in orange). Although dating is sparse for the Essaouira sequences, a Carnian to Norian age for the investigated sandstones is postulated based on biostratigraphic ages from offset wells as well as integration of stratigraphic considerations and the relative position to intercalated dolerites and overlying basalts (CAMP) (see also Fig. 2C). (For interpretation of the references to colour in this figure legend, the reader is referred to the web version of this article.)

Oligo-Miocene, the Essaouira Basin was moderately uplifted and tilted towards the W, which led to widespread erosion of overlaying Cretaceous deposits. To the E, the onshore part of the Essaouira Basin is still buried below younger Mesozoic strata. Uncertainties exist in the thickness and distribution of the (Late) Triassic sequences towards the SE, in direction of the Argana Valley Triassic exposures due to the thick cover of Jurassic and Cretaceous series and the lack of seismic control (e.g. Piqué et al., 1998; Hafid et al., 2000; LeRoy and Piqué, 2001).

4.2. Argana Valley

Extensive exposures of Permian and Triassic sediments are exhibited in the Argana Valley, located along the roughly N-S trending modern day physiographic depression, which runs parallel to the southern extents of the High Atlas mountain chain between Imi N'Tanoute in the N and Ameskroud in the S (Fig. 1). The valley developed during Cenozoic times, when rivers draining southward from the emergent High Atlas eroded through Cretaceous and Jurassic strata, resulting in the exposure of nearly 1500 km^2 of rocks. The Permian to Early Jurassic continental red bed sequence rests unconformably on Palaeozoic sediments, and attain an overall thickness of 4500 m (Duffaut et al., 1966; Tixeront, 1973). The Argana basalt reaches thicknesses of up to 400 m and separates the Permo-Triassic lithostratigraphic members T1 to T8, from the Lower Jurassic units T9 and T10 (AitChayeb et al., 1998; El Hachimi et al., 2011) (Fig. 3). Radiometric ages have been recalculated for basalt flows to 197 ± 0.7 and 201.7 ± 2.4 Ma (Verati et al., 2007) (Table 1), suggesting a stratigraphic age of Sinemurian to Rhaetian calibrated to the timescale of Gradstein et al. (2012), associating them to the CAMP magmatism (Knight et al., 2004; Marzoli et al., 2004; Verati et al., 2007; Deenen et al., 2010). In contrast to the central Essaouira Basin, there is no direct evidence for marine incursions into the Argana area during Upper Triassic or Lower Jurassic times (Hofmann et al., 2000).

Recent structural studies (Baudon et al., 2012; Leleu et al., 2016) highlight dominantly wide-rift or broad sag-basin styles for the eastern provinces, supporting earlier diagnostic work of Hofmann et al. (2000). During the Cenozoic, Alpine deformation caused high-angle faulting in the Central High Atlas, but only minor folding of the Mesozoic sedimentary rocks occurred. The tectonic overprint led to the formation of fault blocks, but in most cases no steep

tilting took place and in general the dip of Triassic strata is less than 30° (Van Houten, 1977; Manspeizer et al., 1978; Manspeizer, 1988, 1994; Beauchamp, 1988; Medina, 1995; Mader and Redfern, 2011; Baudon et al., 2012).

5. Upper Triassic stratigraphy

Dating is a challenge in continental settings, which commonly lack direct biostratigraphic control. Palynological data is sparse, and the only conclusive age data available, that is comparable between the two regions of investigation is presented by the basalt deposits related to the CAMP volcanism. Argana Valley basalt flows yield an absolute age of 197 ± 0.7 Ma and 201.7 ± 2.4 Ma. Within the central Essaouira Basin, dolerite samples from well JRP-1 have an absolute age of 210 Ma (JRP-1: 2768 m, 3163 m from Oujidi et al., 2000) (Fig. 2C). No conclusive ages for the thick flow basalt sequences within the Meskala Field were however available (Fig. 2C). A summary of the stratigraphic framework calibrated by the sparse relative age data is provided for the two areas (Fig. 3, Table 1) to allow for an integrated conclusion on the time-equivalence of the two areas and implications made in view of regional sedimentation patterns.

5.1. Central Essaouira Basin

A tectono-stratigraphic framework for the Essaouira Basin based on seismic interpretation was proposed by LeRoy and Piqué (2001) (Figs. 2B and 3). Within this tectono-stratigraphic framework the Mesozoic sequences were sub-divided into four sedimentary mega-sequences (LeRoy et al., 1997; Manspeizer et al., 1978; Piqué et al., 1998) (Fig. 2B). The lowermost Upper Triassic to Lower Jurassic mega-sequence comprises red, silt-rich clastic deposits, thick evaporites and intercalated basalts, deposited during the syn-rift phase (Piqué et al., 1998; LeRoy and Piqué (2001)). This mega-sequence is composed of three smaller-scale sedimentary sequences. The lowermost sequence sT1 is restricted to a westward tilted half-graben (Piqué et al., 1998; LeRoy and Piqué (2001)), while the second sequence sT2 is thickest along the western border of the half-graben (Fig. 2C). This sequence has been penetrated by well JPR-1, and comprises fluvial sandstones of Carnian age (Piqué et al., 1998; LeRoy and Piqué (2001)) (Fig. 2C). The uppermost unit sT3 overlies an interpreted intercalated basalt and the maximum thicknesses of sT3 can be observed further towards the west (figures 2B,C), highlighting the general westward shift of depo-centres as suggested by Piqué et al. (1998) (Fig. 2B).

In the Meskala Field the Upper Triassic continental facies are overlain by reoccurring mudstones, and approximately 240 m of salt, eventually capped by an approximately 270 m thick basalt sequence (Figs. 2C, 4). A lower Liassic age has been assumed for the salt and mudstone sequences (Hafid et al., 2000; Broughton and Trepanier, 1993; Youbi et al., 2003). The thick basalt sequence can be traced regionally on seismic into the Jeer Field (Hafid et al., 2000) (Fig. 2C) and has also been penetrated by wells in the Meskala Field (Fig. 4). Both, the extrusive basalts, as well as the intrusive sills found within the Upper Triassic deposits (Fig. 2C) are expected to be related to the well documented CAMP event (McHone, 2000; Knight et al., 2004; Nomade et al., 2007; Deenen et al., 2010). The correlation is reinforced by more conclusive biostratigraphic data available for nearby wells MKL-1, where ostracodes of the genus *Darwinula* (between 3027 and 3300 m), and of the genus *Lymnocythere* in MKL-104 (2964 m) (Silmane and ElMostaine, 1997) were recorded, both supporting a Carnian to Norian age in line with the radiometric ages of the basalts. Since the CAMP event is documented to be very short-lived with an

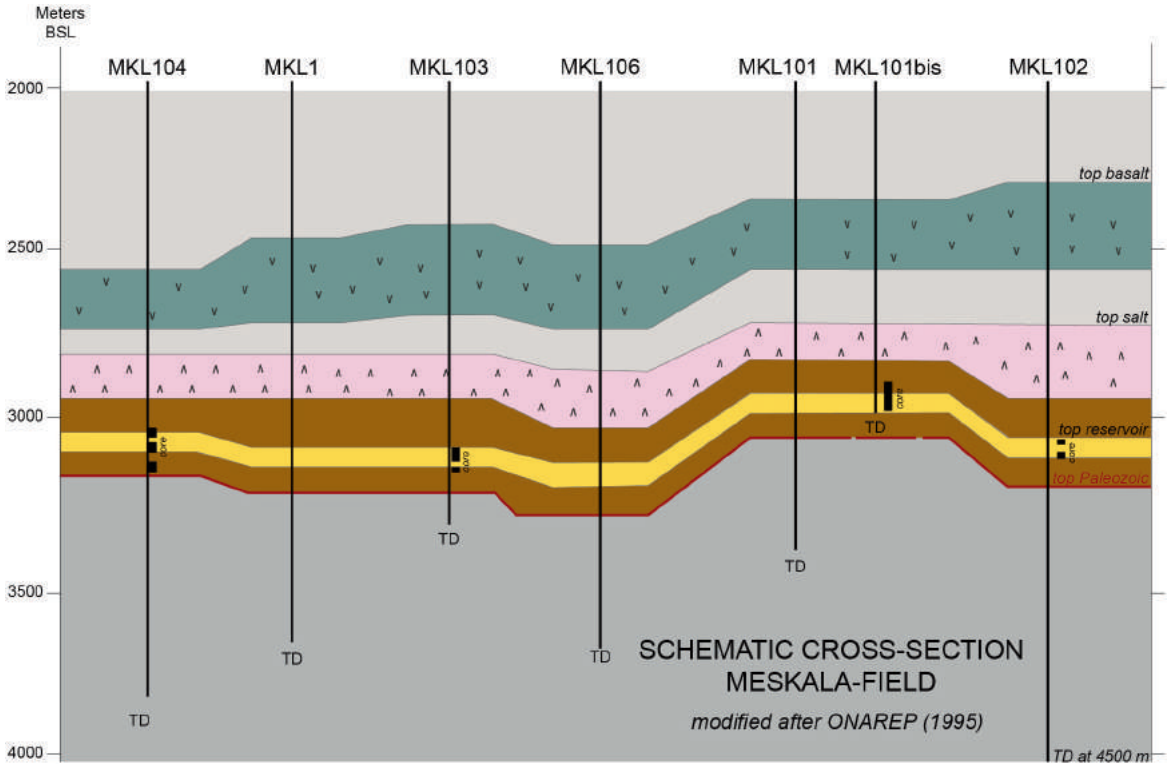

Fig. 4. Schematic cross-section across the Meskala Field, displaying key wells in relation to the reservoir interval (yellow), overlying salt (pink) and basalt (olive green) as well as core availability, location and total depth (TD) of the wells in meters below surface location (BSL) (the exploration wells are close to vertical) (modified after ONAREP, 1995). (For interpretation of the references to colour in this figure legend, the reader is referred to the web version of this article.)

expulsion window as short as 1,5 Ma (McHone, 2000; Nomade et al., 2007), some confidence with respect to the absolute timing is hence placed on the proposed chronostratigraphic framework.

5.2. Argana Valley

The exposed rift-sequences have formerly been divided into the Ikakern, Timezgadiouine and Bigoudine Formations, bound at the top by the Argana Basalt (Duffaut et al., 1966; Tixeront, 1973) (Fig. 3). The formations have further been subdivided into ten lithostratigraphic units numbered T1 to T10 (Tixeront, 1973; Brown, 1980; Hofmann et al., 2000). The Permian Ikakern Formation (T1 and T2) is characterised by alluvial fan and high-sinuosity meander-plain conglomerates with interbedded sandstone and siltstone alternations (Tixeront, 1973; Jones, 1975; Brown, 1980), the Timezgadiouine Formation (T3 to T5) consists of braided or meandering fluvial channels, and cyclical playa deposits (Tixeront, 1973; Brown, 1980; Hofmann et al., 2000). The base of the Bigoudine Formation rests conformably on underlying mudstones and fines, but can locally be unconformable and erosive exhibiting coarse ephemeral alluvial conglomerates (Mader, 2005; Mader and Redfern, 2011). The greatest part of the T6 member however consists of braided river deposits, perennial fluvial sandstones and aeolian dunes (Mader and Redfern, 2011), while the thickest part of the Bigoudine Formation (T7 to T10) displays highly cyclical and laterally extensive playa deposits (mudstones, siltstone, sandstone intercalations) (Tixeront, 1973; Brown, 1980; Hofmann et al., 2000; Tourani et al., 1999). A relatively well constrained biostratigraphic framework was established for the Permo-Triassic Argana Valley sequences combining the work of previous authors with new biostratigraphic data (Jones, 1975; Dutuit, 1976; 1977; Manspeizer et al., 1978; Fiechtner et al., 1992; Tourani et al., 1999, 2010; Jalil and Peyer, 2007; Jalil et al., 2009; Klein et al., 2010, 2011; Verati et al., 2007) (Table 1). The chronostratigraphic framework suggests a Carnian to Norian age for the (uppermost?) T4, T5, T6, T7 and T8 deposits (Fig. 3). Consequently a review of T4/T5, T6 and T7/T8 members is provided in this study in view of major fluvial flow in the Argana Valley analogous to depositional ages anticipated for

Table 1
Compilation of biostratigraphic data and absolute ages available for the Argana sequence. Carnian to Norian deposits time-equivalent to the Meskala field sediments are represented in Argana by members (?T4) T5 to T8 (highlighted by yellow stripy pattern). Where contradicting datums were available, the more unreliable dates are greyed out in the figure and only the best data sets are highlighted in black font for the chronostratigraphic age column (Dutuit, 1988; Hminna et al., 2012; Hunt and Lucas, 1991; Jalil, 1999; Jalil and Dutuit, 1996; Jalil and Janvier, 2005; Lucas, 1998; Voigt et al., 2010).

Member	Author	Vertebrates	Palynology	Radeometric Ages	Chronostratigraphic Age*
Argana Basalt	Verati et al. (2007)			197.8 ± 0.7 Ma 201.7 ± 2.4 Ma	Rhaetian to Sinemurian
	Fiechtner et al. (1992)			K-Ar 205 ± 17 Ma	Norian to Pliensbachian
	Manspeizer (1978)			Ar-Ar 200 to 210 Ma	Rhaetian to Norian
T8	Tourani et al. (1999)		Assemblages similar to T7 with very good *Camerosporites secatus* and abscense of *Corollia/Classopollis (11)*		11 Earliest Norian (or younger)
T7	Tourani et al. (1999)		*Patinasporites densus (6) Paracirculina quadruplicis (10) Camerosporites secatus (9) Spiritisporites spirablis (8)*		10/9 Late Carnian to Early Norian 8 Late Carnian (Tuvalian)(or younger)
T6	Tourani et al. (1999)		*Pseudoenzonalasporites summus (7) Patinasporites densus (6)*		7 Late Carnian (Tuvalian) to Norian 6 Carnian to Middle Carnian
T5	Dutuit (1976, 1977); Jalil & Dutuit (1996); Hunt & Lucas (1991); Lucas (1998)	*Phytosaurs* (A) *Paleorhinus magnolucus (5), Angistorhinus talainti* *Metoposaurs* (B) *Metoposaurus azerouali* *Dicinodonts* (C) *Moghreberia nmachouensis* (Otischalkian Landfaunachron)			5 Late Triassic; 5 Paleorhinus-biochron (Pangaea): Late Carnian (Tuvalian) A/B/C Assembleage: Carnian to Upper Carnian
	Tourani et al. (1999)		*undated; poor data recovery*		
	Jalil (1999)	Phytosaurs, Metopausaurs, Aetosaurs and *Placerias*-like forms			Carnian (Middle to Late Carnian) resembles Upper Triassic European and American assemblages: *no distinct dating!*
T4	Jalil (1999)	*Capitosauris* remains *Cyclotosaur (x)*			
T3	Jones (1975); Tourani et al. (2010) Klein et al. (2011)	Chirotherioid traces (1) *(Synaptichnium, Chirotherium, Brachychirotherium, Isochiotherium)*		Volcanics: 247±15 Ma (2); 280±15 Ma (3), 300±15 Ma (4)	Olenekian (1) *(Middle Triassic (2); Permian (3) Upper Carboniferous (4))*
T2	Dutuit (1988); Jalil & Dutuit (1996); Jalil (1999); Jalil & Janvier (2005); Voigt et al. (2010); Hminna et al. (2012) Klein et al. (2010)	*Diploid* amphibians *(A) Diplocolus minimus* *Chaptorinid* reptiles *(B) Moradisaurinae* *Diplocaulida, Capthorinida, Pareiasauria, Hylodichnus, Pachypes, Amphisauroposus; Eretopus, Dromopus*			Upper Permian; Permian (Ufimian-Kazanian)(A/B)
T1	Jones (1975)			Volcanics in conglomerates 247±15 Ma	Upper Permian to Middle/Lower Triassic
					* *calibrated to Gradstein et al. (2012)*

the Essaouira sequence in the Meskala Field.

6. Core and facies analysis: central Essaouira Basin, Meskala Field

Core analysis of wells from the Meskala Field was undertaken (this study) and results were subsequently compared to outcrop data and literature from the Argana Valley. An almost fully cored section from well MKL101*bis* is presented and discussed in terms of the sedimentological evolution of the basin. MKL101*bis* was chosen as the example well, as it contains the most continuous Triassic section cored in the Meskala Field (Fig. 4). It hence offers the possibility to study a continuous vertical Triassic profile without major gaps. The generalised facies associations resulting from this work are under-pinned by additional wells. In total ten litho-sedimentary facies (*sub-facies*) were identified and combined into four facies associations (FAs) (Table 2). Facies associations of well MKL101*bis* are discussed from base to top, the core is described with absolute thickness in centimetres, and core gaps were noted where present (Figs. 5–10). The detailed facies description and interpretation for the core intervals is provided in Tables 2–5, while in the following a brief summary of the facies associations is provided.

6.1. Summary facies associations

Facies Association 1 (FA1) consists of three *sub-facies* and is dominated by very fine to fine grained sandstones (Table 3; Fig. 5). Finer material is sparse, but minor amounts of clay can be found in the form of thin (<10 cm) mudstone horizons. Sedimentary structures include horizontal or low angle stratification (Fig. 9A), massive bedding or inverse grading. Secondary angular cavities (<1 cm in diameter) were abundant within this sandstone dominated unit. The facies association was interpreted to represent ephemeral fluvial braided river deposition in transition to a wet aeolian sandflat environment (Table 3).

FA2 comprises four *sub-facies* and is dominated by compound, well-sorted, very fine to fine-grained sandstone units interbedded with thick mudstone intervals (Table 4; Fig. 6). The thickness of individual sandstone packages ranges from approximately 50 cm to up to 4 m, with interbedded dark red to purple mudstone units up to 2 m thick, and minor siltstones interspersed. The ratio between sandstone and mudstone dominated intervals is approximately 3:2, and sediments of FA2 were interpreted to represent perennial fluvial channels with adjacent floodplain fines (Table 4).

FA3 contains three *sub-facies* (Table 5; Figs. 7, 8), which are

Table 2
Summary of facies associations and related litho-sedimentary *sub-facies*. Both, description and interpretation of the main depositional units are provided in the table. More detailed descriptions and depositional environment descriptions are summarised in Tables 3–5, and illustrated in Figs. 5–10.

Facies Association (FA)	Sub-Facies Code *(sfa)*	Description	Depositional Environment/Interpretation sub-facies		Climatic Implications
			Sfa	FA	
FA 1	*1a*	Vfs; minor sltst-mdst; horizontal to low angle stratification; minor ripple stratification; massive; colour change from grey to red; angular dissolution	Ephemeral fluvial channels	Ephemeral fluvial braided river deposition transition to wet aeolian sandflats	periodic arid-humid changing to dominantly arid
	1b	Mixed grey vfs-fs, vfs; finely laminated to adhesion ripple cross-stratified and mottled (rooted?); winnowing; reworked material; abundant secondary angular dissolution	Channel abandonment facies (paleosols, rooting, deflation)		
	1c	Fs; well sorted; horizontally laminated; well cemented; patchy pink cement (anhydrite?); winnowed; distinctively orange coloured	Wet aeolian sandflats		arid
FA 2	*2a*	Intercalated mdst-sltst; horizontal lamination or highly destratified; dark red to purple; minor vfs-fs in form of ripples interbedded	Floodplain deposits	Perennial fluvial channels with floodplain deposition	humid in hinterland, periodic arid to humid in depositional setting
	2b	Vfs-fs; horizontal lamination to low-angle; or massive to destratified; well cemented; pink colour; fining upward sequences	Fluvial channels (perennial)		
	2c	Clast dominated conglomerate; dark grey or red/purple mudstone rip-up clasts; vfs-fs sst matrix; interbedded with dark-grey mudstones	Sheet flood/splay deposits		
	2d	Mdst; black; enriched w organic material; minor sltst interbedded (ripples)	?Lacustrine/Playa lake shales		
FA 3	*3a*	Vfs-fs; medium steep to massive destratified; remnant horizontal, wavy laminations; abundant water escape structures and syn-sedimentary faulting; erosive bases with reworked material	(Fluvial) Channels/Delta top (destratified)	Fluvial delta plain to delta top deposition	humid in hinterland, periodic arid to humid in depositional setting
	3b	Vfs-sltst; fining-upward cycles; well preserved horizontal lamination and ripple-cross bedding; thin mudstone horizons and clay drapes are intercalated; locally minor bioturbation	Delta plain/Delta top with delta mouthbars		
	3c	Sltst-mdst; red to purple; massive; alternating with black mdst enriched with organic debris; inter-bedded vfs ripple cross-stratification; abundant water escape structures; calcretes	Delta top transition to playa (floodplain)		
FA 4	*undivided*	Mdst; dark red to purple; minor sltst; mottled; minor horizontal lamination	Playa mudstones	Playa deposition	arid

Table 3
Detailed descriptions and summary interpretation for Facies Association 1 with sub-ordinate *sub-facies 1a* to *1c*. The deposits of this FA are interpreted to report ephemeral fluvial, braided river deposition in transition to a wet aeolian sandflat environment and abandonment of the system (Fig. 11A). A summary log with typical lithological characteristics of this facies association is in addition displayed in Fig. 5.

FA1 Sub-Facies Code (*sfa*)	Description	Interpretation: Ephemeral fluvial braided river deposition in transition to wet aeolian sandflats
1a Ephemeral fluvial channels	Sub-facies 1a consists of moderately well-sorted, very fine-grained, horizontal to low-angle stratified reddish grey sandstones (Fig. 5). They often appear massive or destratified and are very well cemented. Typically up to three 1 m–2 m thick sandstones were recognised throughout the cores. There is an apparent increase in destratification up section. The sandstones are often capped at the top by a thin (<10 cm) black to dark grey mudstone horizon. Silt or finer sandstones can be interbedded with the mudstones in form of thin ripple- or horizontal lamination. The intercalated mudstones show a distinct colour change from dark grey and black to dark red up section. Angular cavities seemingly unrelated to primary stratification can be abundant.	The dominance of horizontal to low-angle stratification, the sheet-like character with sharp top and basal contacts and the overall lack of fine material are interpreted to represent sheetflood fluvial deposition during repeated discharge events (Miall, 1977, 1996, 2006; Fisher et al., 2008; Anderson et al., 1999). No clear erosive bases or higher angle cross-bed sets which would point to deep, confined channels were recognised, and deposition in a non-confined braided river system is inferred (Miall, 1977, 1996, 2006; Bridge, 1993; Bridge, 2003, 2006). Occasional interbedded thin mudstone horizons that cap these well sorted sandstones are interpreted to be genetically linked and record deposition from suspension during low-energy flow conditions of waning flow (Miall, 1977; Turnbridge, 1981; Kumar et al., 1999; Newell et al., 1999; Platt and Keller, 1992; Owens et al., 1999; Bridge, 2003, 2006). Massive sandstones defined by prominent destratification and minor remnant faint patchy lamination often associated with these deposits, are hence interpreted to represent post-depositional modification and dewatering during abandonment. Finer, often ripple-laminated sandstones, were mainly recognised at the tops of individual packages, and associated to bedform migration by unconfined tractional flow while lower flow regime conditions prevail (e.g. Jopling and Walker, 1968).
1b Channel abandonment facies (paleosols, rooting, deflation, etc.)	This sub-facies consists of alternations of very fine to fine-grained sandstones that are either a) light grey and horizontally laminated, b) greyish to red with adhesion ripple stratification, c) dark grey, horizontally laminated, with abundant angular cavities, or d) dark red with wavy to horizontal lamination and a mottled (rooted?) appearance. Additionally, thin (<10 cm) dark grey mudstones with abundant organic debris and coaly fragments may be interbedded. Individual bed thickness is centimetre to decimetre scale, and the sediments appear generally very mottled, disrupted and destratified. The sub-facies is further characterised by abundant secondary dissolution cavities.	The mixed interval of *sub-facies 1b* is characterised by sedimentary structures related to exposure, where highly mottled sediments as a result of rooting or disrupted stratification due to evaporation processes are common. Adhesion ripple stratification as well as interbedded sandstones with sharp top and basal surfaces suggest periodic deposition. Reworked organic matter and organic clasts are also present, and the development of a weakly developed immature palaeosol is hence proposed (Retallack, 1988).
1c Wet aeolian sandflats	*Sub-facies 1c* consists of fine-grained, very well-sorted, exclusively horizontally laminated sandstones, which are less well cemented in comparison to the deposits of *sub-facies 1a* and *1b*. The stratification is very well preserved, and distinct inverse grading is characteristic. The very well sorted sandstones lack any fine material, and they are defined by a discrete colour change to orange-pink, that corresponds with the occurrence of patchy pink (? anhydrite) cements.	These deposits above an internal bounding surface are generally slightly coarser and appear winnowed, displaying inverse grading. The sandstones show a marked colour change to orange-pink above the immature paleosol. Concurrently, the interbedded mudstones exhibit a change in colour from grey-black (suggesting reducing conditions) to red (oxidising conditions). The dominance of horizontally bedded inverse stratification in the sandstones is interpreted to highlight the transition from a shallow braided fluvial system *(sfa1a)* to a wet aeolian sand-flat environment (*sfa1c)*, dominated by fluctuating water tables in a semi-arid to arid environment (e.g. Kocurek and Nielson, 1986; Kocurek, 1988).
Secondary processes	Angular cavities are distinctive in this FA and overprint a variety of *sub-facies*. The cavities are angular and typically <2 cm in diameter. In the sandstone dominated part of *sub-facies 1a*, they initially don't appear to be related to depositional sedimentary structures. However, they show an association with facies where primary lamination is strongly altered by dewatering processes. Considered in context to the overall depositional environment, the cavities could represent ghosts of clay rip-up clasts along the bases of braided fluvial sheet flood units or shallow channels. In *sub-facies 1b* similar dissolution cavities are concentrated to specific horizons. These deposits were instead interpreted as immature paleosols, and the cavities are proposed to record dissolution of an early calcite cement, or gypsum layers related to evaporation and subsequent capillary groundwater processes (Retallack, 1988).	

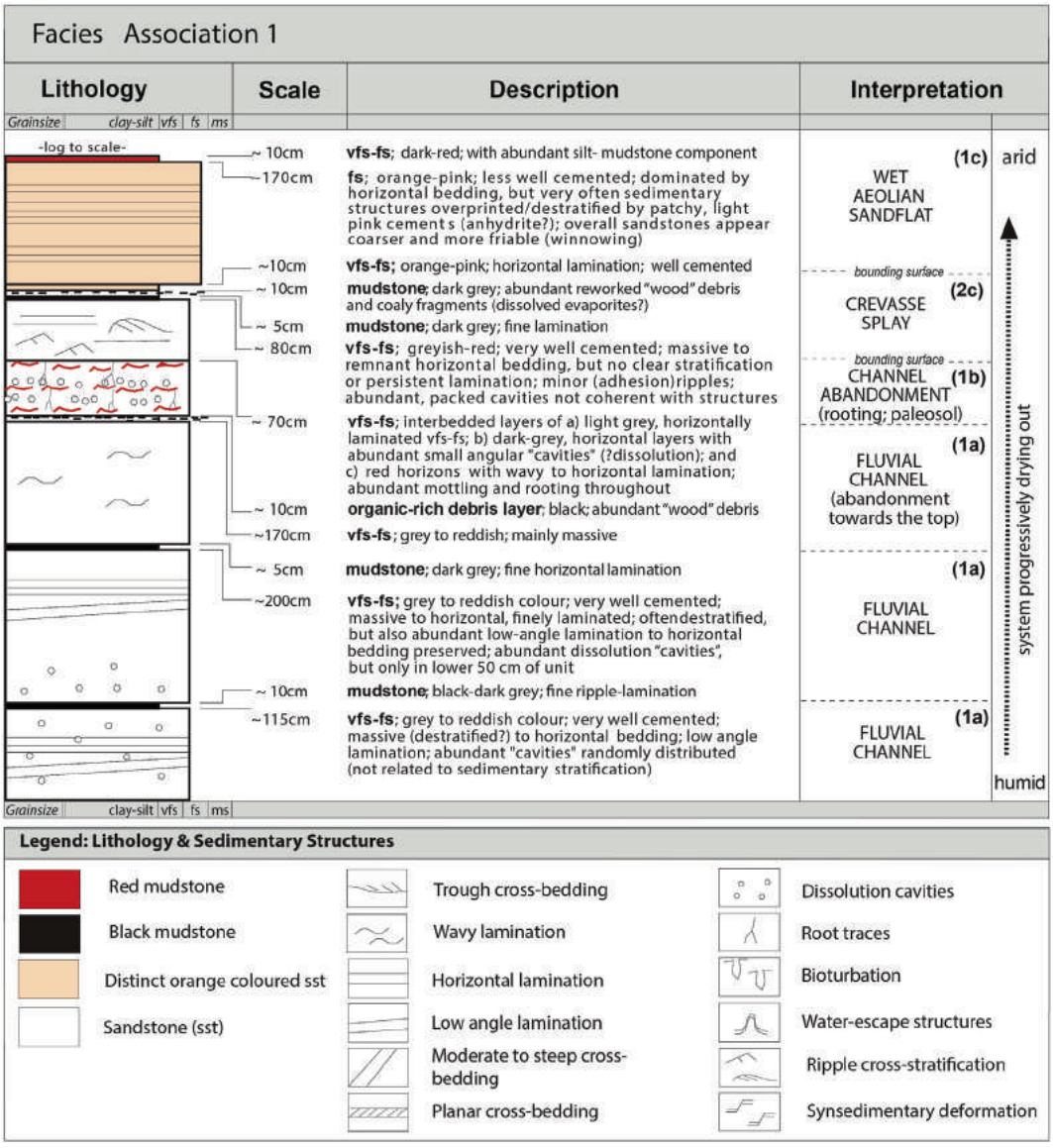

Fig. 5. Lower 8,65 m of cored section from MKL101*bis*. This part of the core exhibits facies association 1 (FA1) with detailed description of grain size, sedimentary structures, colour and cementation if apparent. In the interpretation column, the facies interpretation (*sub-facies* code) is displayed, whereas the detailed interpretations for this FA are summarised in Table 3. The deposits of this facies association were interpreted to represent ephemeral shallow braided river deposits, with abandonment of the system towards the top and a transition into a wet aeolian sandflat environment. The legend provided for this figure is applicable for Fig. 5–10. (For interpretation of the references to colour in this figure legend, the reader is referred to the web version of this article.).

repeated in three distinct fining-upward cycles. The two lower cycles, consist of 8–10 m thick sandstone dominated fining-upward sequences, while the upper cycle exhibits about 4–5 m thickness (Figs. 8 and 10). Each fining upward cycle features a sharp, locally erosive basal contact, and the sandstones are interbedded with minor mud- to siltstone intervals (Figs. 7, 8 and 10). Overall, FA3 is dominated by fine to very fine-grained, ripple cross-bedded to less abundant massive or destratified sandstones. Calcretes or coaly interbeds are abundant, and the sequences is generally overprinted by root traces or mottling throughout. Dewatering structures and wavy horizontal lamination are abundant, and only remnant horizontal to low-angle lamination can be observed in the sandstones. Overall, a transition from fluvial delta top to shallow ?lacustrine or playa lake delta deposition is suggested (Table 5).

In contrast to the sandstone dominated FA1 to FA3, FA4 is dominated by dark red to purple, mottled mudstones which can change progressively into dark red to purple silt- to mudstones with minor horizontal or wavy-horizontal lamination, regularly reverting back to cleaner mudstone intervals (Table 5; Fig. 8). Minor very fine to fine grained sandstone intervals are interbedded in the form of small-scale (<1 cm) adhesion ripple stratification. Unlike the lower units and mudstones interbedded in the sandstone dominated FA2 and FA3, no intercalated dark grey to black mudstone intervals or thicker (>1 cm) sandstone intervals were observed. Full playa deposition with little clastic input to the system is hence anticipated (Table 5).

7. Depositional model Essaouira

Taking into account the climatic overprint inferred from sedimentary structures recorded in core, a progressive evolution from

Table 4
Detailed descriptions and summary interpretation for Facies Association 2 with sub-ordinate *sub-facies 2a* to *2d*. FA2 was interpreted to represent perennial fluvial conditions with extensive floodplain deposition and associated creveasse splay deposition (Fig. 11A). A summary log with typical lithological characteristics of this facies association is in addition displayed in Fig. 6.

FA2 Sub-Facies Code (*sfa*)	Description	Interpretation:Perennial fluvial channels with floodplain deposition
2a Floodplain deposits	*Sub-facies 2a* consists of dark red to purple mudstones with minor siltstone or fine grained sandstone intercalations. Particularly where silt- and sandstones are interbedded, horizontal or wavy as well as ripple lamination is observed. The fine grained sandstones often consist of centimetre-scale single ripple trains forming beds up to 2 cm. In general the mudstones appear highly destratified. Small rootlets were recognised as well as dewatering structures. The mudstone dominated intervals are up to 2 m thick. Towards the top of the section slickensides were observed.	Above a major bounding surface, sedimentary facies changes (Fig. 6) into several meter thick compound sandstone intervals (*sfa2b*), interbedded with several meter thick, dark red to purple mud-siltstone units *(sfa2a)*. The upward-fining sandstone units are interpreted to represent fluvial channels (*sub-facies 2b*) within an extensive floodplain environment (*sub-facies 2a*) (e.g. Miall, 1996; Nanson and Croke, 1992; Kumar et al., 1999; Newell et al., 1999; Colombera et al., 2015). The intercalated very fine-grained sandstone deposits are up to 4 m thick, and are suggested to represent both amalgamated sheet-like sandstone elements, and more confined (crevasse) channel deposits (Nanson et al., 1986; Miall, 1996; Bristow et al., 1999; Bridge, 2003; Medici et al., 2015). In general it can be noted that silt- to sandstone material is commonly interbedded with the mudstones, suggesting frequent low-energy flood events with non-confined flow during times when fluvial discharge exceeds the systems capacity (Bridge, 2003, 2006; Cain and Mountney, 2009).
2b Perennial fluvial channels	This sub-facies comprises of very fine to fine grained (0.088–0.177 mm), very well sorted, well cemented, horizontal to low-angle laminated grey to light pink coloured sandstones (Fig. 9A). The sandstones are also massive or destratified in part. Locally, moderately steep cross-bedding, particularly along the basal contacts of individual sandstone packages are apparent. These thick clastic units range between 150 and 400 cm, exhibiting fining-upward from fine to very fine sst and sltst with an increasing mud component. The upper parts of the fining-upward sequences can be dominated by ripple laminations and are often mottled and destratified along their top boundaries.	
2c Sheet flood or splay deposits	This lithofacies comprises of clast-rich conglomerates consisting of dark grey or red mudstone rip-up clasts and minor organic debris within a very fine silt- to very fine to fine grained sandstone matrix (Fig. 9B). Individual beds are up to 50 cm thick, have an erosive base and sharp top, and can locally be interbedded with dark grey mudstone layers. In the mudstones abundant mud-filled simple burrows were recognised. The burrows are mainly vertical from the top surfaces down, with diameters of <0,5 cm and vertical length of 1–2 cm.	Conglomeratic, sharp based and possibly sheet-like deposits of *sub-facies 2c* are interpreted to represent overbank, splay and sheetflood deposition. They become more prominent up section, which could suggest progradation of the crevasse splays.
2d Lacustrine/Playa shales	Up to 40 cm thick organic-rich black mudstone horizons, interbedded with thin siltstone intercalations featuring minor wavy to fine ripple lamination.	The top bounding surface of this sequence is marked by the deposition of a 40 cm thick black mudstone horizon *(sub-facies 2d)*. A transgressive event, related to expansion of a shallow (playa) lake, or alternatively the development of laterally extensive inter-pond area on the floodplain with reducing conditions is anticipated (e.g. Wright and Mariott, 1993; Mariott and Alexander, 1999; Bridge, 2003). For both scenarios high groundwater tables are a prerequisite.

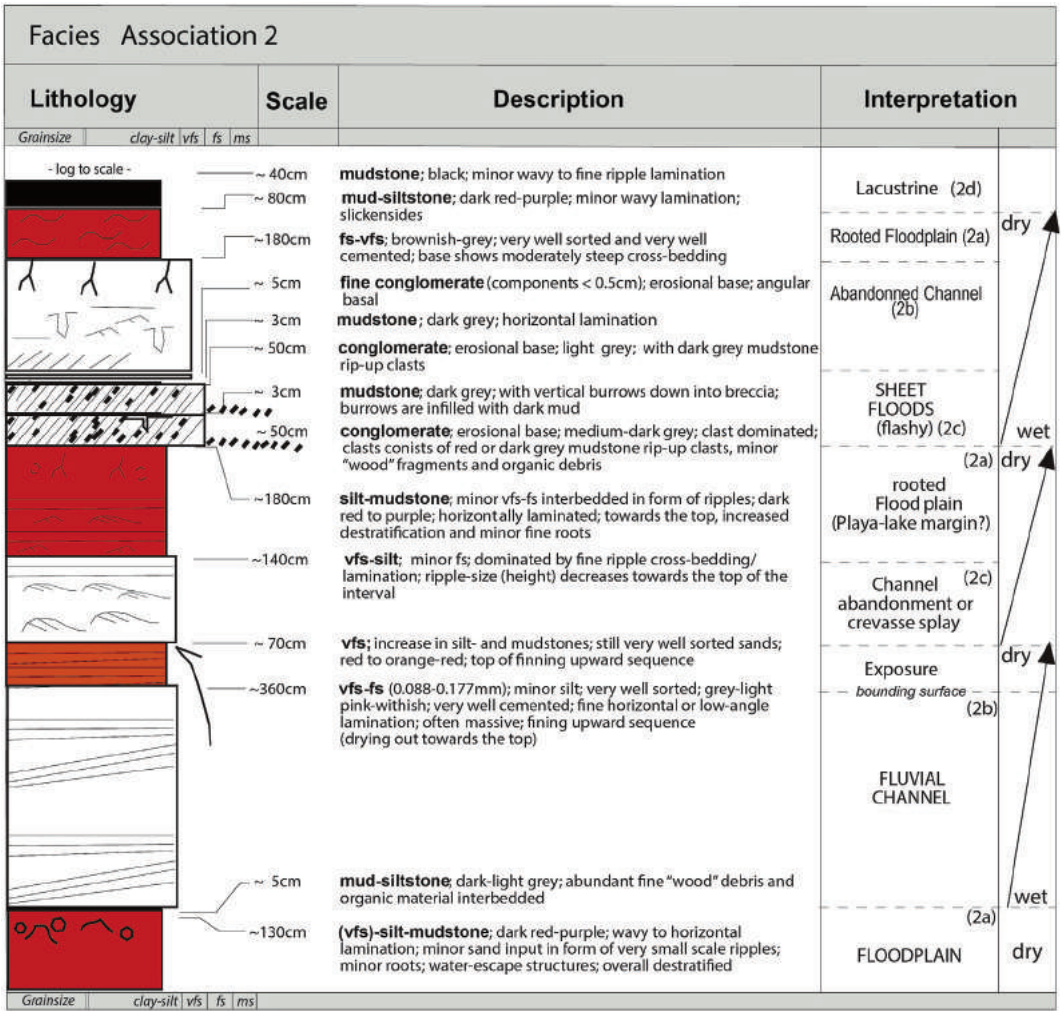

Fig. 6. Above a 40 cm core gap to the basal part of the core in MKL101*bis* (Fig. 5), the 13,46 m described display facies association 2 with detailed description of grain size, sedimentary structures, colour and cementation if apparent. The facies interpretations for FA2 are summarised in Table 4 and were interpreted to represent deposition in a perennial fluvial environment with extensive floodplains and associated crevasse splay deposition (for lithology legend see Fig. 5). (For interpretation of the references to colour in this figure legend, the reader is referred to the web version of this article.)

FA1 to FA4 suggests the following major depositional stages:

- **FA1**: ephemeral braided river deposition to wet aeolian sandflat environment (Fig. 11A);
- **FA2**: perennial fluvial deposits with extensive floodplain fines (Fig. 11B);
- **FA3:** fluvial deposits in transition to a shallow lacustrine delta environment with distributary mouthbars and cyclical abandonment of the fluvial facies (Fig. 11C);
- **FA4**: playa environment with extensive, highly mottled mudstones.

With the exception of FA1 and FA4, the main reservoir intervals comprise stacked fining-upward sequences interbedded with thick, occasionally organic-rich mudstones (Figs. 10 and 11). The sandstones in FA1 differ from the overlying sandstone deposits of FA2/FA3 by being slightly coarser in grainsize, less well sorted, lacking fines and exhibiting a different fluvial style. The FA1 sandstones are typically horizontally laminated and imply sheet-like deposition with a high relatively well sorted sandstone content and little fines (Fig. 11A). The lack of fines is assumed to be related to proximity to source, but could also imply lateral confinement (e.g. Wright and Mariott, 1993). Overall, the sandstones of FA1 were interpreted to represent episodic discharge in a shallow braided river system (Fig. 11A), and in comparison to FA2 and FA3 a more proximal depositional setting is proposed. Within FA1 an obvious change from dark grey mudstones enriched with organic matter, to dark red to purple, often mottled mudstones was observed. While the presence of organic matter implies vegetation and humid conditions to transport and preserve the plant material, the shift from overall reducing to oxidising conditions is inferred from the colour change. More humid conditions, at least in the catchment area, are therefore proposed for the lower part of the system, but a shift in local climate to more arid (oxidising) conditions is apparent. Abandonment of the fluvial system is suggested, marked by an immature paleosol implying an extended time of exposure (*sub-facies 1b*). Above this internal bounding surface, a phase of amplified aridity is interpreted to have led to the development of a wet aeolian sandflat environment (*sub-facies 1c*). Increased winnowing of the sandstones, a dominance of horizontally bedded and inverse graded deposits suggest augmented evaporation processes with fluctuating groundwater levels. This interpretation is supported by the recognition of a patchy anhydrite cement overprinting *sub-facies 1c*. This type of cementation has previously been associated

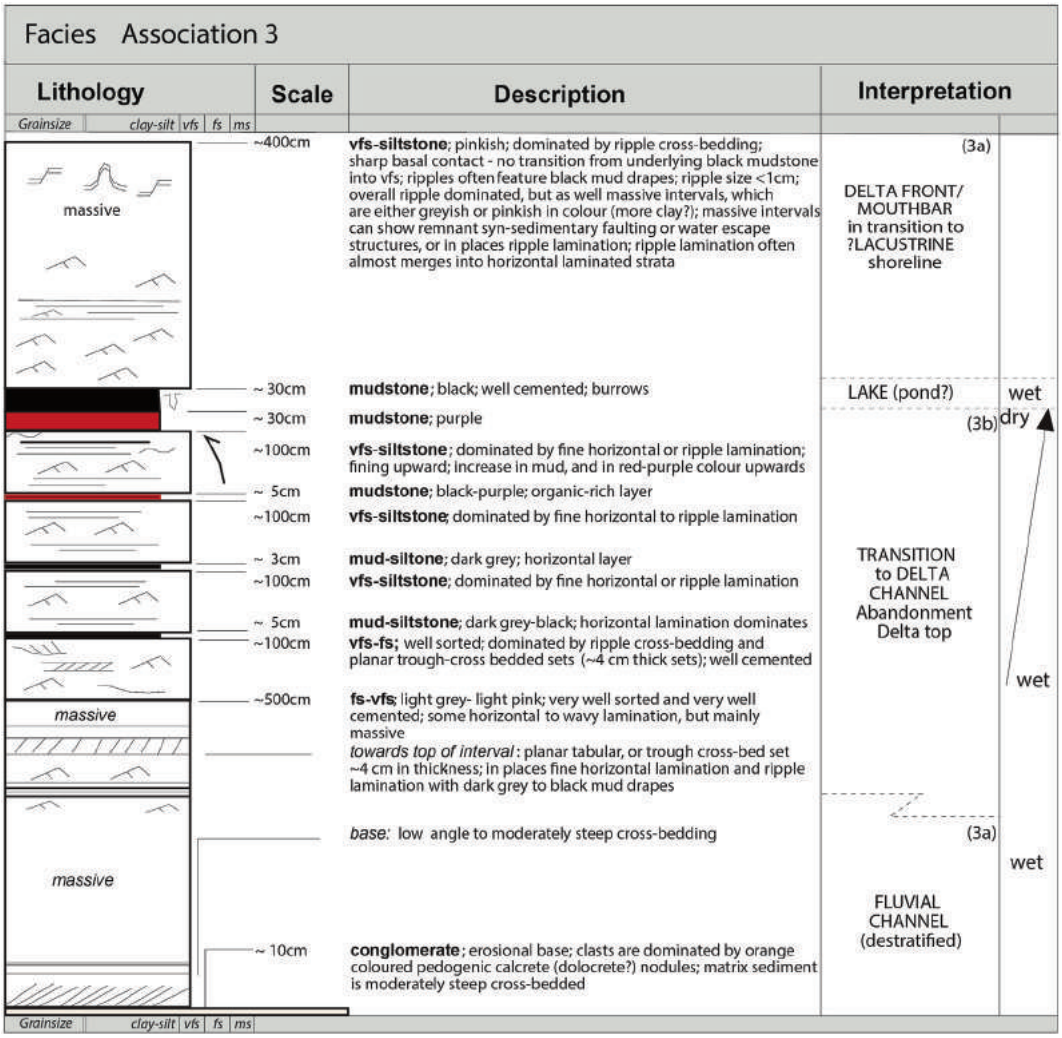

Fig. 7. In these 13,83 m of core from MKL101*bis*, facies association 3 is described (continued in Fig. 8). The sediments of this facies association were interpreted to be deposited in transition from a fluvial environment to a delta environment with distributary mouthbars, characterised by the abundance of ripple cross-stratification and coaly interbeds. Delta top facies with organic-rich mudstones, paleosols and rooting is observed (for lithology legend see Fig. 5). The detailed interpretations for this FA are summarised in Table 5.

with alternating groundwater levels, where above the groundwater table in the presence of saline waters and evaporation, the anhydrite is precipitated in form of patchy cements in an overall arid setting (Glennie, 1970).

A prominent change in depositional environment from sheet-like ephemeral flow to metre-scale fluvial channel deposits and abundant, thick floodplain fines succeeds FA1 (Fig. 11B). Several fining-upward sequences of well sorted, very fine grained sandstone packages associated with extensive dark red mudstones are documented (FA2). A fluvial setting with abundant crevasse splay and overbank deposition within laterally shifting facies belts associated with the migration of channels within an extensive floodplain environment is proposed (e.g. Miall, 1996) (Fig. 11B). The fining-upward profiles may reflect cycles of increased water availability and discharge, or simply lateral autocyclic migration and avulsion of the system. Extensive dewatering of the sediments and syn-sedimentary faulting observed in these units however implies relatively oversaturated sandstones, possibly related to more humid conditions. The increased influx of water to the area may has further led to a raised groundwater level, which favoured the dissolution of early calcites or evaporates indicated by the angular cavities prominent in FA1. The colour of the interbedded floodplain fines points towards overall oxidising conditions, however where deposition was rapid, preservation of dark black mudstones, deposited under reducing conditions is possible. Alternatively, shallow semi-permanent lakes on the floodplain could be envisaged. The presence of reworked organic-rich to almost coaly reworked deposits in an overall oxidised floodplain environment is thus interpreted to suggest cyclical shifts between humid and more arid conditions, whereby the humidity could have been restricted to the catchment area.

The fluvial deposits become increasingly interdigitated with transgressive deposits, suggesting the expansion of an adjacent shifting shoreline (FA3) (Fig. 11C). Each of the fining-upward sequences exhibits deposition of dark grey or black organic-rich mudstones at the top (Fig. 10) interpreted to document the direct influence of a longer-lived shifting shoreline. These black organic-rich deposits change in composition throughout the interval, from organic-rich mudstones with organic wood-plant debris <40%, to coaly layers composed of 80–100% organic material, towards the top. The sandstones change from clearly defined fluvial channel deposits to dominantly ripple cross-stratified sandstones with abundant organic-rich to almost in-situ coal beds. The environment of deposition changes into a delta setting with

Table 5
Detailed descriptions and summary interpretation for Facies Association 3 and 4 with sub-ordinate sub-facies 3a to 3c.The deposits of FA3 were interpreted to consist of fluvial delta plain to delta top deposits in a shallow (playa) lake environment (Fig. 11C), whereas the mudstone dominated FA4 was interpreted to highlight full playa conditions. A summary log with typical lithological characteristics of these facies associations are in addition displayed in Figs. 7 and 8.

FA3 Sub-Facies Code (*sfa*)		Description	Interpretation: Fluvial to delta plain and delta top deposition
FA 3	*3a* (fluvial) Channels to delta top (destratified)	*Sfa3a* is on first account very similar to *sub-facies 2b*, characterised by moderately steep cross-bedded or massive, destratified very fine to fine grained sandstones which are light grey in colour. Thicknesses of individual sandstone units are comparable (up to ~4 m), but in contrast to *sub-facies 2b*, the basal contacts of *sub-facies 3a* are often erosive and basal contacts contain reworked material, such as calcrete (?dolocrete) nodules (Fig. 9C). The reworked nodules are orange to whitish in colour and typically <1 cm in diameter, aligning with the foresets of the medium steep cross-bedding.	Above a black shale marker horizon, two to three fining-upward sequences were recognised that comprise 70–80% of FA3 (Figs. 8 and 10). Both fining-upward sequences consist of moderately steep cross-bedded to massive deposits (*sub-facies 3a*) in the lower part, transforming into ripple cross-stratification interbedded with thin organic-rich mudstone intercalations in the upper part (*sub-facies 3b*). Sedimentary evidence is ambiguous, and sedimentary features could record similar facies previously described in crevasse splay deposits and lacustrine deltas (Miall, 1996; Bridge, 2003). Certainly in the lowermost sequence investigated in the core, the erosive based, moderately steep cross-bedding with abundant reworked coarse material suggests an erosive channel base and large scale dune migration from traction currents. As flow wanes, abandonment of the system would lead to extensive ripple laminated strata as observed. However, the entire second finning upward cycle is dominated by ripple-cross stratification throughout, featuring abundant climbing ripple trains above a sharp but non erosive basal contact. The abundance of organic material interbedded further suggests transition into a more lacustrine delta depositional environment, with subaqueous levees or delta-mouthbar deposits (e.g. Miall, 1996; Bridge, 2003).
	3b Delta plain or delta top and delta front mouthbars	*Sub-facies 3b* is dominated by very fine grained sandstones to siltstones with very well-defined and well-preserved ripple cross-stratification, planar trough-cross bed sets and minor horizontal lamination or massive appearance. The ripple facies consist of stacked, small scale (2–4 cm) planar cross-bed sets with s-shaped foresets, and finer material lining the latter (Fig. 9D). Individual ripples are low relief, often <1 cm, almost merging into horizontal lamination. The ripple cross-stratified sandstones are either intercalated with thin (~5 cm thick), dark grey mudstone-siltstone horizons, or abundant thin, black, organic-rich mudstone layers with a coaly character (Fig. 9C). Locally, small vertical burrows and rootlets intersect the mudstones. Water-escape structures and syn-sedimentary faulting appear throughout. The upper 2 m–4 m of each fining upward cycle are dominated by this sub-facies.	
	3c Delta top in transition to playa (floodplain)	This sub-facies shows similarities to *sub-facies 2a*, with heterolithic deposits characterised by up to 3 m thick mudstone-siltstone-sandstone packages. The mudstone intervals are overprinted by an abundance of rootlets and highlight an overall mottled appearance as in *sub-facies 2a*, but the reddish background facies can in contrast be interbedded with dark grey to black mudstones enriched with organic debris (up to 5 cm large clasts). In addition, up to 30 cm thick layers packed with orange coloured calcrete (?dolocrete) nodules (<1 cm) were observed (Fig. 9D). The interbedded coarser material is defined by sharp basal contacts, that are typically ripple cross-stratified and massive to destratified with visible water-escape structures towards their top contacts. The orange coloured nodules do not follow any obvious bedding, but are concentrated in packed layers with little matrix surrounding them.	At the base of the lower fining-upward sequence (Figs. 8 and 10), the occurrence of reworked orange-coloured pedogenic nodules suggest the development of palaeosols (calcrete/?dolocrete) (Retallack, 1988; Khalaf, 2007) within the adjacent floodplain or delta top. In the upper fining-upward sequence in-situ calcrete nodules were recognised. In these sediments primary stratification of the host sediment is distorted and sedimentary structures indicative of reworking and flash-flood deposition are lacking, confirming the preservation of more mature paleosols in the system. In addition, the upper part of each cycle contains abundant organic-rich layers, adhesion ripples, mottling and rooting, interpreted to represent periodic exposure, following either a shifting lake shoreline or simply lateral channel switching on the flood or delta plain.
FA4 Sub-Facies Code (*sfa*)		Description	Interpretation: Playa Fines
FA 4	Playa deposits	The FA is dominated by dark red to purple, mottled mudstones which can change progressively into dark red to purple silt- to mudstones with minor horizontal or wavy-horizontal lamination, regularly reverting back to cleaner mudstone intervals. Minor very fine to fine grained sandstone intervals are interbedded in the form of small-scale (<1 cm) adhesion ripple stratification. In contrast to the lower units and similar mudstones observed in FA2 and FA3, no intercalated dark grey to black mudstone intervals or thicker (>1 cm) sandstone intervals were observed.	The dominance of dark red mudstones is interpreted to represent full playa conditions (e.g. Hofmann et al., 2000; Arche, 2007). Repeating shallowing and subsequent drying of the playa is indicated by an increase in mottling and rooting and the abundance of adhesion ripple stratification. Destratification and water-escape structures are common and the deposits show a high degree of exposure (e.g. Nanson et al., 1986; Hofmann et al., 2000).

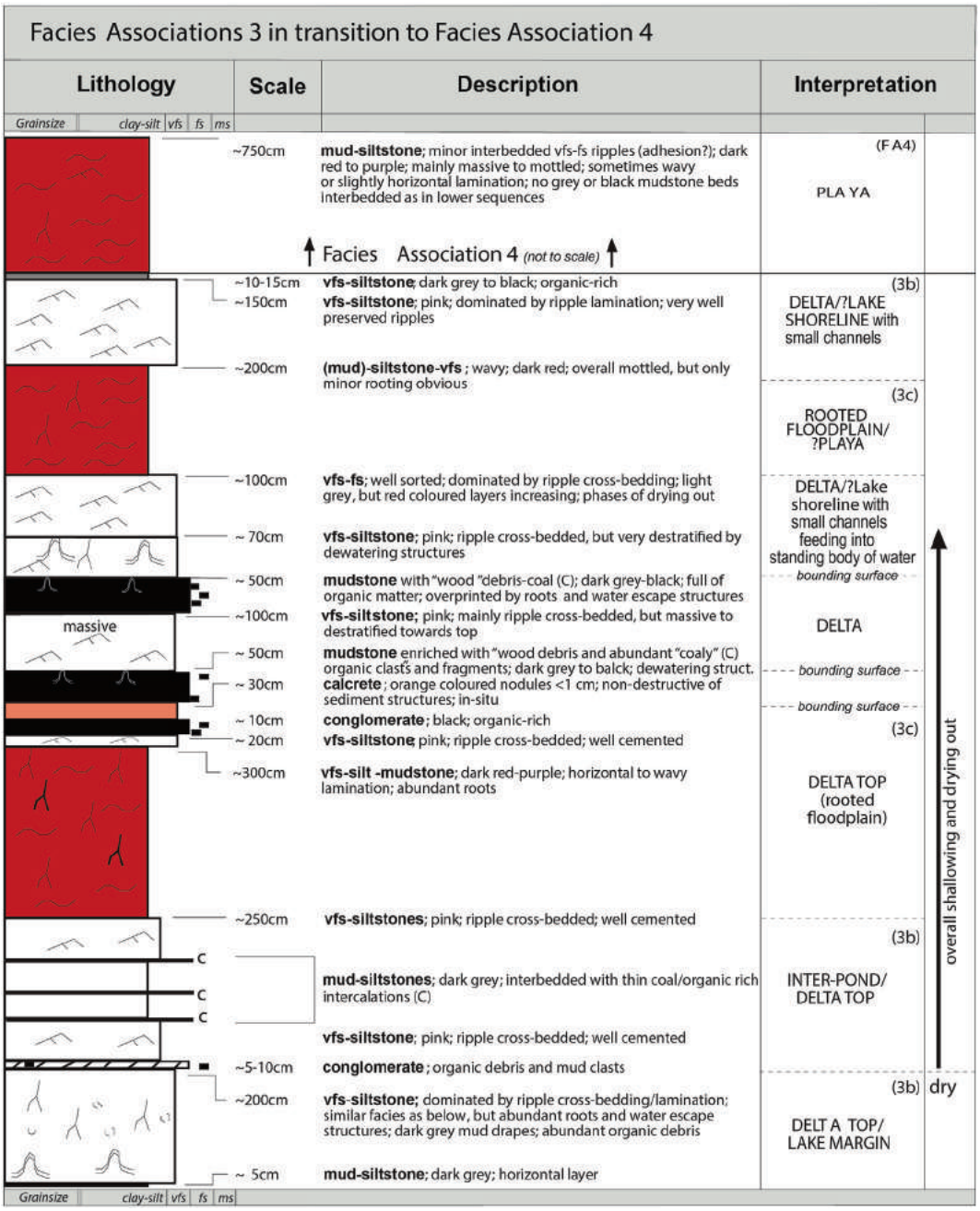

Fig. 8. Summary description of facies association 3 and 4 (15, 60 m). The sediments of facies association 3 were interpreted as delta top sediments with abundant organic-rich mudstones, paleosols, small channel or splay deposits and a high amount of rooting and mottling. The upper 7,5 m of core represent facies association 4, and are interpreted to exhibit full playa conditions under dominantly reducing conditions (note that FA 4 is note presented to scale) (for lithology legend see Fig. 5). The detailed interpretations for these FA are summarised in Table 5.

distributary mouthbars and abundant inter-pond areas (Fig. 11C), with more permanent water available. Simultaneous with the increase in organic matter to the system, the input of sandstones seems to decrease considerably. This decrease in clastic input could be an effect of numerous scenarios: less fluvial input related to decreased run-off and possibly an increase in aridity in the hinterland (Schumm, 1968; Smoot, 1991; Shanley and McCabe, 1994; Howell and Mountney, 1997; Blum and Tørnqvist, 2000; Nanson et al., 1998), a less efficient hinterland source (e.g. Leleu and Hartley, 2010), or simply basin closure and back-filling or back-stepping of the system (e.g. Schumm, 1993). While an increase in humidity would be inferred from the high amounts of organic matter present, strong evidence for increased aridity is provided by the paleosols observed in the system. The formation of these nodular calcretes requires sufficient precipitation to translocate the carbonate, but equally prerequisites high evaporation rates (Reeves, 1976). Typically they form during arid to semi-arid intervals following humid periods (Wright, 1992; Alonso-Zarza, 2003), or alternatively, calcretisation takes place in the vadose zone within the floodplain during arid climates (Wright, 1992; Wright and Marriot, 1996; Alonso-Zarza, 2003; Khalaf, 2007). Both processes imply rather arid climates, which is also reflected in the increased destratification and related evaporation processes recognised in the host rock towards the top of the sequence. An increase in aridity,

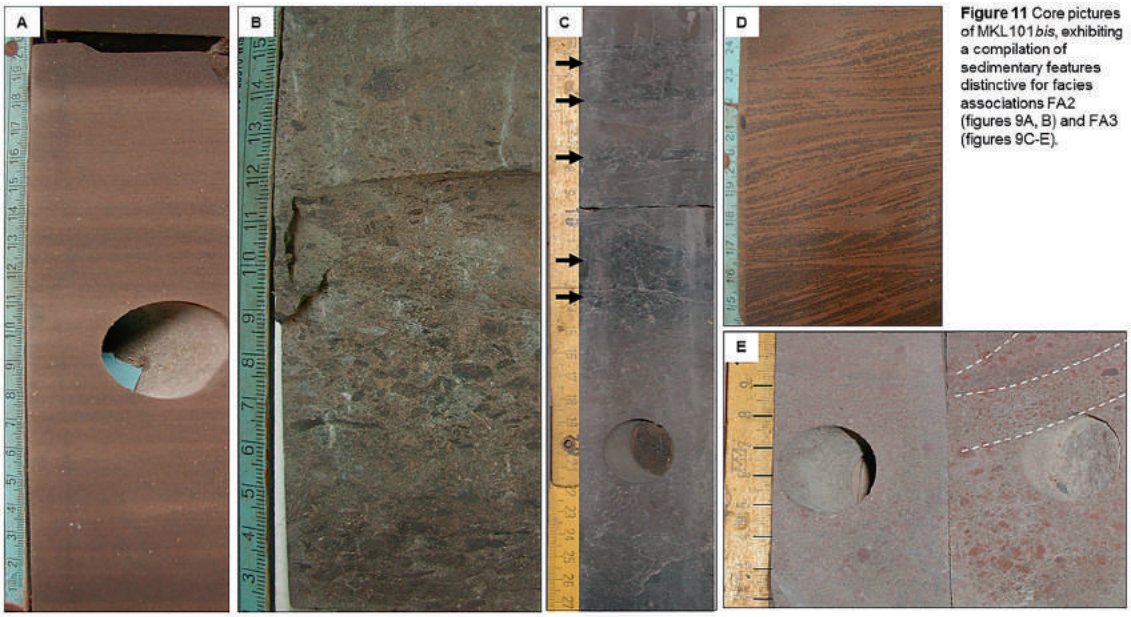

Figure 11 Core pictures of MKL101*bis*, exhibiting a compilation of sedimentary features distinctive for facies associations FA2 (figures 9A, B) and FA3 (figures 9C-E).

Fig. 9. Core pictures of MKL101*bis*, exhibiting a compilation of sedimentary features distinctive for facies associations FA2 (Fig. 9A, B) and FA3 (Fig. 9C–E).

possibly within a system that still promotes high groundwater tables is therefore envisaged, and a combination of basin closure and changes to the prevailing climate back to more arid conditions is suggested.

Gradually, towards the top of the logged section, the input of coarser sandy material ceases entirely, and an extensive playa environment with dominantly oxidising conditions, governs the last phase of deposition (FA4). Arche (2007) reviewed the appropriate use of the term playa, concluding that subsurface hydrogeology, evaporite geochemistry and tectonic regime are crucial to accurately define a particular playa or sabkha setting. With respect to the investigated deposits it remains open to discussion whether the term playa, i.e. deposits of continental dry depressions, versus sabkha defined as marine saline flats along arid shorelines is appropriate, as the exact nature of the shoreline could not be distinguished during this study. The sedimentological data suggests shifting shorelines, and only minor amounts of evaporite deposits were recognised. However, thick salt deposits of marine origin overlay the investigated deposits (figures 2B,C, 4), which certainly suggest marine incursion at a later stage. But since no direct marine indicators were recognised in the investigated deposits, a rechargeable or through flow playa system (Arche, 2007) with possibly a well-developed playa lake remains the preferred interpretation for the studied interval (FA4).

8. Discussion: regional impact

The Argana Valley is located approximately 80 km SE of the Meskala Field (Figs. 1, 12), where Carnian to Norian continental deposits (T4/5, T6, T7/T8) have been studied in outcrop by several authors (Tixeront, 1973; Jones, 1975; Brown, 1980; Hofmann et al., 2000; Tourani et al., 2010; Mader and Redfern, 2011). In the past, the Argana sequence has been proposed to represent the proximal equivalent of the prolific reservoirs in the central Essaouira Basin (Brown, 1980; Broughton and Trépanier, 1993; Hafid et al., 2000).

Owing to the lack of extensive subsurface and seismic data it is not possible to correlate directly between the Argana Valley exposures and the central Essaouira Basin subsurface section, thus these conclusions have been largely based on assumptions of structural trend predictions and limited paleocurrent data (e.g. Tixeront, 1973; Brown, 1980; Medina, 1991, 1995). Our study focuses on the sedimentological and climatic evidence from Carnian to Norian deposits in both areas, and conclusions that might be drawn from the sediments preserved. For the purpose of this comparative study, a synopsis of sedimentological work with emphasis on major fluvial flux in the Argana Valley as well as the concurrent climate is presented.

8.1. Literature review of Carnian to Norian deposits (?T4/T5, T6, T7/T8), Argana Valley

Based on Duffaut et al. (1966), Tixeront (1973) and Jones (1975) early work, Brown (1980) generated a synopsis on the tectono-stratigraphic evolution of the Argana Valley (Figs. 3, 12). In terms of facies distribution, Brown (1980) summarises the T4/T5 member as floodplain deposits with intercalated meandering river sandstones, T6 is described as a deltaic complex with westward prograding delta-mouth bars, and T7/T8 were attributed to delta-plains and mud-flats with distributary channel deposition. Field measurements of flow directions led Brown (1980) to the conclusion that all sediments in the Argana Valley are initially derived from the E, and distributed towards the W following E-W trending basement faults (Fig. 12). He emphasises the predominance of normal faulting and suggests that some of the structures in the lower units functioned as tilted fault blocks, which influenced lateral sediment distribution throughout deposition of the entire Triassic sequences. Measurements for the Timezgadiouine (T4/T5) and Bigoudine Formation (T7/T8) led Brown to conclude that sediment dispersal is imposed by the Tirkou and Timezgadiouine horst (Fig. 12), diverting sediments S and N into the grabens respectively. Within the grabens paleocurrents are towards the W. Although not explicitly discussed, the measurements published by

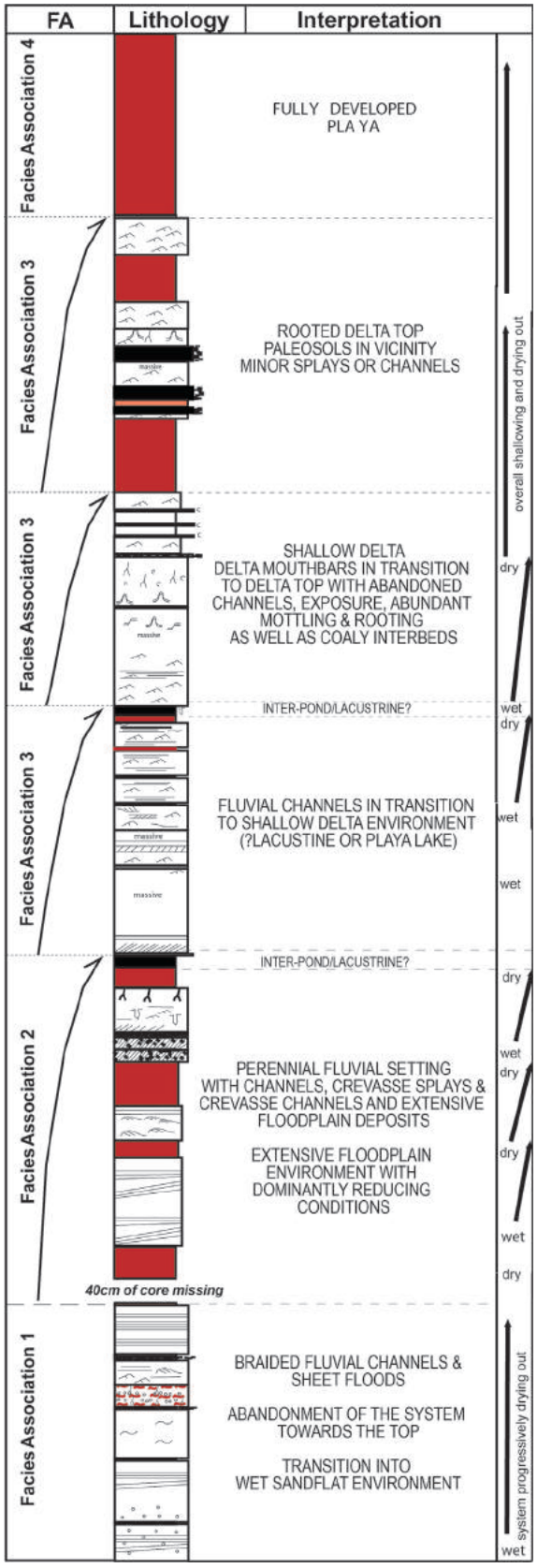

Fig. 10. Simplified summary litholog, documenting sedimentary facies associations and interpretation of the major sequences recognised across the Meskala Field using MKL101*bis* as an example. The core spans close to 60 m, with a minor core gap of 40 cm in the lower part of the well (see also Fig. 4 for position within the well). The continuous core was interpreted to represent a progressive evolution from an ephemeral fluvial to wet aeolian sandflat system. A marked change in fluvial depositional style and architecture from sandrich, shallow, sheet like ephemeral channels to larger, perennial fluvial channels with extensive rooted floodplains and paleosols is apparent. Reducing conditions are dominant in the accumulation area, even though the fluvial style and accompanying deposits suggest more perennial, possibly humid conditions. This more perennial fluvial system further develops into a shallow delta setting that is progressively followed by extensive playa deposition under reducing conditions.

Brown (1980) clearly highlight a prominent S to SW component in addition to westerly trends, both in the Timezgadiouine and the Bigoudine Formation (Fig. 12). Hofmann et al. (2000) presented detailed sedimentological work with a focus on paleoclimate in view of observed cyclicity, sediment accumulation history and basin evolution of the mudstone dominated sequences T4, and T7 to T10. Their work focuses on the mudstone dominated units and highlights a great degree of lateral continuity of cyclical mudstones deposits throughout the basin. The interbedded sandstone dominated facies has been described as unconfined sheetfloods, possibly related to ephemeral meandering streams (T4), a mixture of sheetflow deposits, often affected by haloturbation, sheet delta deposits with mud-draped wave ripple lamination, mixed fluvial aeolian massive deposits overprinted by haloturbation, and purely aeolian cross-bedded deposits interbedded with thick mudstone-claystone alteration of an arid saline shallow ephemeral lake environment (T7/T8). Hofmann et al. (2000) did not provide flow directions for any of the sandstone dominated facies, however highlights a general trend of progressive thickening and coarsening of the sandy facies. This coarsening upward trend is ascribed to a basinward migration pattern driven by a gradual climatic drying. Moreover, Hofmann et al. (2000) stresses the lateral continuity of T4, T7-T10, which they attribute to shifting facies belts between a marginal to a more central basinal position. A very flat basin topography is suggested based on the lateral extend of aeolian marker beds. Hofmann et al. (2000) further states that based on the cyclical stacking pattern, the extensive lateral extent of individual cycles and sheet-like character structural movement can be discounted. The observed cyclicity was assigned to oscillatory fluctuations in paleoclimate instead, and an overall drying upward cycle, which generated fluctuations in the playa basin driving lateral shifts in sediment distribution was hence suggested.

8.2. Field study of T6, Argana Valley

An extensive field study (Fig. 12) focusing on the sandprone Tadrat Oudaou Sandstone member (T6) was carried out by Mader and Redfern (2011), who presented a comprehensive sedimentological model. Two main phases of sediment flux to the Argana Valley during T6 times were proposed, interrupted by a phase of pronounced aridity throughout the basin (Figs. 13–17). The early fluvial phase documented represents a coarse ephemeral alluvial fan to braidplain setting (Figs. 13, 14 and 17A), characterised by high amounts of channel switching and restriction to the centre of the Argana Valley exposures (Fig. 12, locality 1, 2). Extensive flow directional measurements suggest dominantly E to W flow with sub-ordinate SE to NW flow directions (Figs. 12 and 14). Remnant aeolian deposits as well as products of aeolian deflation are commonly interbedded throughout. Towards the W (Fig. 12, locality 2), in flow direction of the conglomeratic facies, the fluvial deposits display a mere thickness of 2 m, which was attributed to reflect pinch-out of the system toward W and NW (Fig. 17A).

The second major fluvial phase, characterised by highly aggradational, and more perennial fluvial deposition, extensively distributed and exposed throughout the Argana Valley (Figs. 15–17B). The size and internal complexity of individual

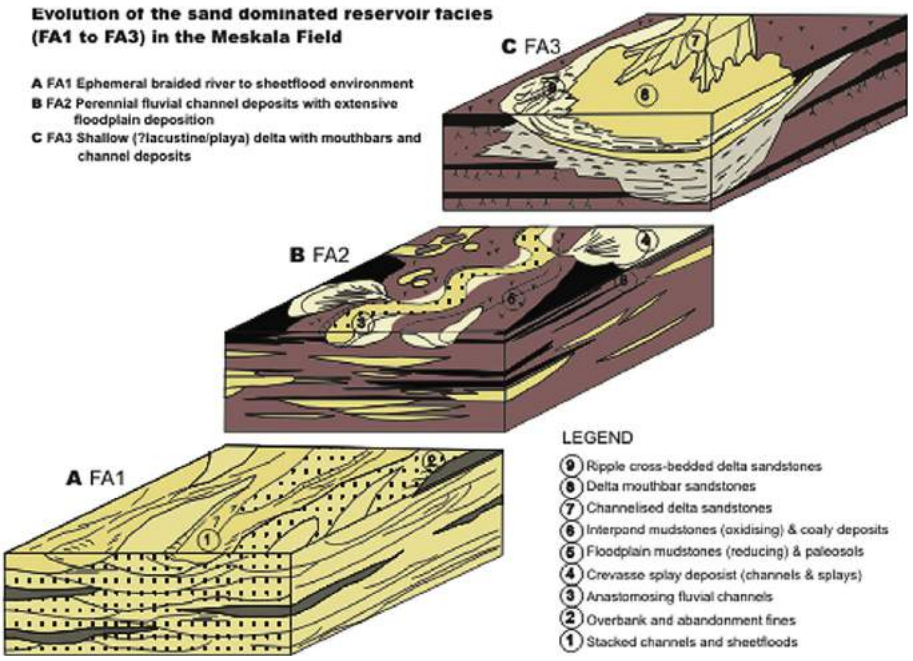

Fig. 11. Depositional model for sediments investigated in core from the Meskala Field. The figure displays the major depositional units summarised in FA 1 (A), FA2 (B) and FA3 (C).

channels suggests a relatively long-lived fluvial system (Figs. 13A and 15). During this late fluvial phase flow directions of fine grained perennial channels are predominantly from N to S in both the northern most locality (Fig. 15A) and the southernmost locality (Fig. 15B). The southernmost locality (figures 12, locality 4) was interpreted to have acted as a major depo-centre for the basin, with maximum thicknesses of T6 preserved (up to 70 m) (Fig. 15B). E to W flow directions were established for the central locations (Fig. 12, locality 1), and a N-S running axial drainage system, fed by fluvial tributary systems from the E (for example in central Argana, locality 1) feeding the southern and southwestern Argana realm during this depositional stage was suggested (Figs. 14 and 17B). Subtle changes in basin geometry affect spatial variations and facies variability throughout. The fluvial system is terminated along a sharp extensive upper bounding surface and the onset of aeolian sedimentation (Mader and Redfern, 2011), which is subsequently transgressed by lacustrine mudstones of the T7 member (Hofmann et al., 2000).

8.3. Implications for regional sediment distribution

While growth faults are reported by Brown (1980) and Medina (1991, 1995) to be common, neither Hofmann et al. (2000), Mader and Redfern (2011) nor Baudon et al. (2012) recognise strong evidence for syn-sedimentary fault control during the Upper Triassic. Minor faults were attributed to dissolution of evaporites and linked collapse features (Hofmann et al., 2000). Mader and Redfern (2011) highlight the possibility of limited fault controlled accommodation space only for the basal early fluvial phase in the centre if the Argana Valley (Fig. 12, locality1), but point out that accommodation space equalised during the late fluvial phase of T6, and that facies distribution observed is a consequence of laterally shifting facies belts driven by the local climate rather than tectonic movement. Baudon et al's. (2012) work suggest that the prominent NNE striking faults are post-depositional, and Hofmann et al. (2000) further concluded that sedimentary cycles observed within the Carnian to Norian T4, T5, T7 and T8 members related to a flat basin topography were correlatable with identical thickness over several 10s of kilometres. Baudon et al. (2012) who contributed the most recent structural review for the area, highlights the impact of the Massif Ancien as a potential structural buffer between the Central High Atlas to explain the slower subsidence observed, and suggests a wide sag-basin type geometry for the Late Triassic section in the Argana Valley rather than narrow half-graben settings. This uncharacteristic broad basin morphology has further been documented on seismic lines in the Central Essaouira Basin (Hafid et al., 2000), and is supported by a recent regional review of the Atlantic margin by Leleu et al. (2016). Both, the recent sedimentological and structural studies suggest that during Carnian to Norian times equalisation of accommodation space prevailed, and that the influence of deep seated structural highs as well as E-W trending basement faults had little to no influence on sedimentation as previously suggested (e.g. Brown, 1980; Laville and Petit, 1984; Medina, 1991, 1995). The main driving factor for the cyclicity observed were climate related, while lateral sediment distribution was attributed to autocyclic processes with fluctuating facies belts and compensational shifting (Hofmann et al., 2000; Mader and Redfern, 2011).

Paleocurrent flow measurements from Brown (1980) and Mader and Redfern (2011), show two dominant directions of fluvial flow for the Timezgadiouine (T4-T5) and Bigoudine (T6-8) Formations:

a) E to W flow direction;
b) NE-SW and/or N to S.

Whilst an E-W paleocurrent component is prominent along the easternmost exposures, closest to the Eastern basin bounding margin, the Western exposures record a prominent N-S and NE-SW direction (Figs. 12 and 17). A distributary system, feeding a southerly accommodation sink is suggested, not one focusing flow to the present day central Essaouira Basin in the NW (Meskala Field) (Fig. 1), casting further doubt on the model proposed by Brown (1980), Broughton and Trépanier (1993) and Hafid et al. (2000) who tentatively identified the Triassic sequence of the Argana Valley as the direct sediment provenance for the central Essaouira Basin.

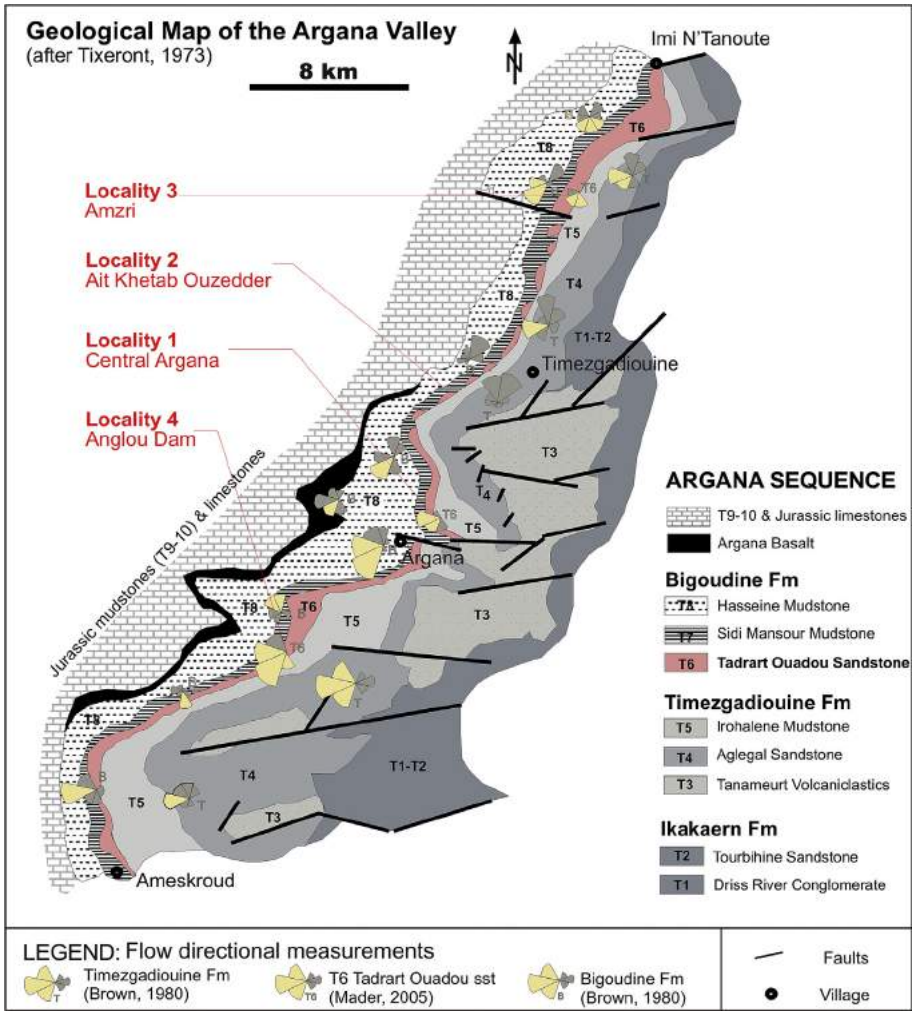

Fig. 12. Geological map of the Argana Valley displaying the lateral distribution of Permian to Lower Jurassic members and formations between Imi N'Tanoute in the North, and Ameskroud in the South. Structural elements (major faults as defined by Tixeront, 1973) are added. An overlay with flow directional measurements from Brown (1980), Mader (2005) and Mader and Redfern (2011) for Carnian to Norian sequences is provided. Study localities 1 to 4 of the outcrop work from Mader (2005) and Mader and Redfern (2011) are marked in red. (For interpretation of the references to colour in this figure legend, the reader is referred to the web version of this article.)

Although the comparison of the Carnian to Norian sedimentary facies suit in the Argana Valley and the Essaouira Basin in context to common basin models (e.g. Matthews and Perlmutter, 1994) could suggest a direct proximal-distal relationship, regional sedimentological evidence is conflicting. For example, for deposition of T6 (Argana Valley) a model scenario could be envisaged, where T6 represent the proximal to mid-distal end member, and deposits from the central Essaouira Basin exhibit the transition from the mid-distal to distal playa (?lake) end member. To further use T6 fluvial deposits as a model scenario, a sediment fairway with direct SE to NW fluvial flow from Argana to Essaouira would be required to specifically feed the accommodation space in the Meskala Field following this direct source to sink relationship (Fig. 1). While general facies distribution fits the model, field evidence from the Argana Valley of T4/T5, T6 and T7/T8 (Brown, 1980; Mader and Redfern, 2011) suggests, that direct SE to NW fluvial flow was only recognised close the easterly expected bounding fault entry points (Brown, 1980; Mader and Redfern, 2011), and subordinately for the early alluvial phase of T6, which is anticipated to be laterally restricted to central Argana Valley (Fig. 17A). Instead, S/SSW flow directions dominate along the western most exposures (Fig. 12), and both Brown (1980) and Mader and Redfern (2011) indicate increased accommodation space in the S. The onset of regionally extensive, isopachous lacustrine and playa strata of T7 to T10 (Hofmann et al., 2000) would typically be interpreted as widespread post-rift sedimentation with major fluvial input to the system terminating in a closed basin setting. Leleu et al. (2016) point out that within wide rift-basin geometries, the onset of lacustrine strata could also fall into the late syn-rift stages of basin evolution, hence imply continued subsidence and accommodation space creation. A potential exit point for sediments in a fill and spill scenario would hence be the S, or SW/W (Fig. 1). The next 'sink' towards a southerly direction is the Souss Basin (Fig. 1), where thick Triassic deposits have been confirmed by drilling. Dependant on basin geometries towards the SW/W, interconnection and cross-basinal flow of sediment, changing flow direction from S to N in the newly developing western extensional basins, and then leading into the central Essaouira Basin area, would have to be envisaged (Fig. 1). This scenario would be analogous to fill and spill models for Triassic rift systems such as the Sherwood sandstone in the UK for example (Wills, 1970; Audley-Charles, 1970). With the progressive westward shift of active rift development in SW Morocco (LeRoy et al., 1997) a scenario where sediment is "stored" in the southern Argana or Souss Basin, later subsequently recycled and transported axially along the rift to the N through the newly developing western extensional basins, could be imagined. A certain

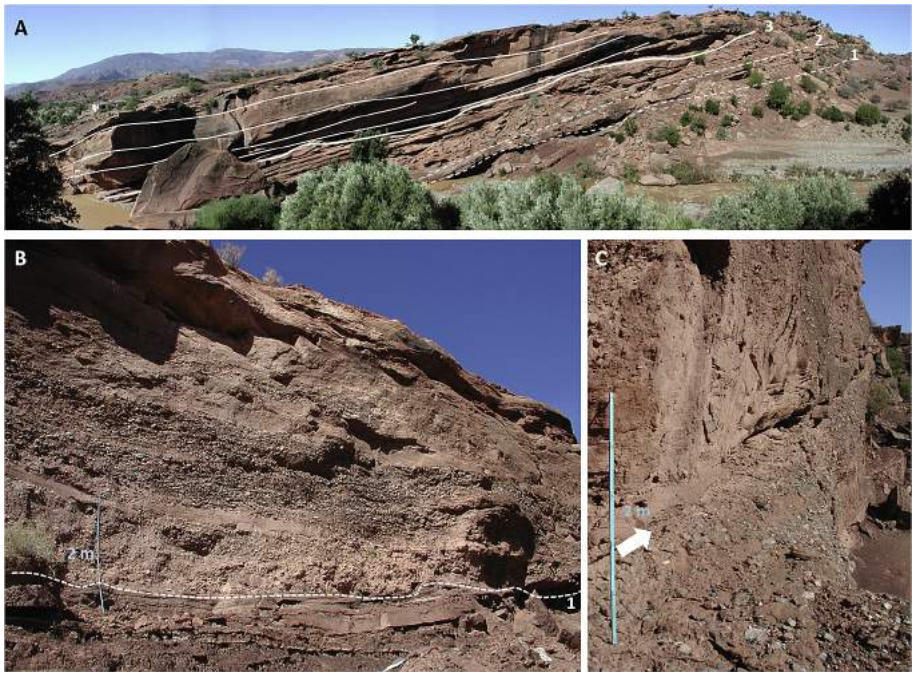

Fig. 13. Overview on fluvial deposits exposed in the Argana Valley (Fig. 12, locality 1). **13A** Roughly N-S trending ridge exposes the early and late fluvial phases. The base of T6 (1 - white dashed line) in this locality is erosive and unconformable on underlying mudstones of T5. The early fluvial phase (white dashed line, interval between lines 1 and 2) thickens towards the N and pinches-out towards the S, thinning from 2 m to 0.5 m along this part of the outcrop over a short distance. The base (interval 3, white line) of the late fluvial phase incises deep into underlying floodplain fines of the early fluvial phase. The channels show large-scale cross-bed sets up to 2 m thick. **13B** Coarse pebble conglomerates with minor amounts of fine material, highly erosive, characterise the early fluvial phase (scale bar 2 m). **13C** Deposits of this early fluvial phase thicken from the exposure in 13A of 1 m, to more than 10 m within ~1 km distance. A sharp internal bounding surface (white arrow) can be recognised over several hundred metres, which could suggest some degree of confinement.

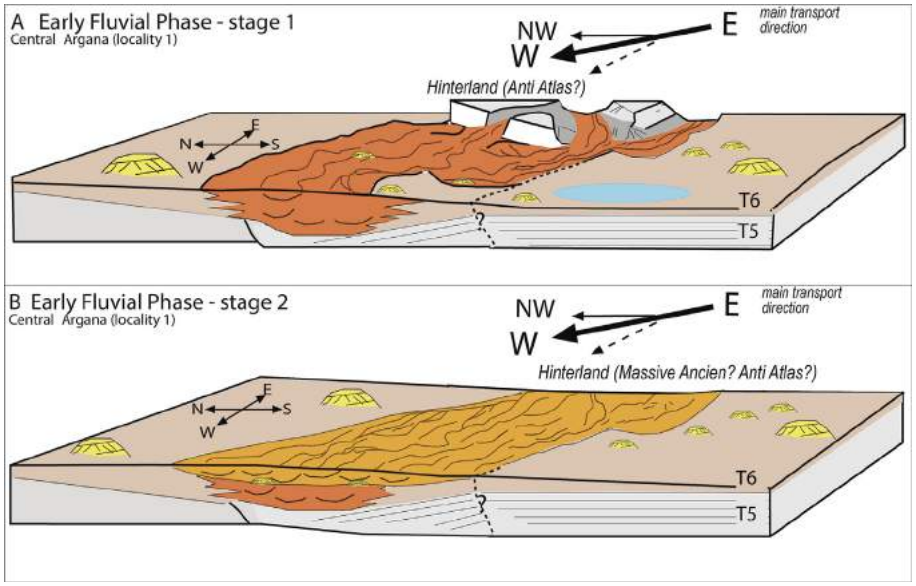

Fig. 14. Simplified two stage depositional model for the early fluvial facies as recognised in locality 1 (Argana). **14A** Infill of early accommodation space by coarse alluvial fans and braided rivers. The deposits pinch-out to the S, and the main transport direction is towards the W, subordinately NW, with an easterly hinterland source. **14B** The figure highlights the progressive deposition of the low-sinuosity braided river system, sourced from the E. A likely hinterland source could be presented by the Anti Atlas or the Massiv Ancien further in the NE.

diachronism between the source and sink would however have to be expected in this scenario.

The continuous evolution from proximal fluvial facies to distal delta or playa lake end member conditions in the Meskala Field presented in this study, are however anticipated to suggest a more local source to sink relationship. The Central Jebilet Massif located in the NW (Fig. 1) could present a more local hinterland source instead, or, similar to speculations for the Argana sediment routing (Mader and Redfern, 2011), the Anti Atlas could be envisaged as the easterly hinterland source. Further regional provenance studies are required to reconstruct the Triassic hinterlands of Morocco with refined precision.

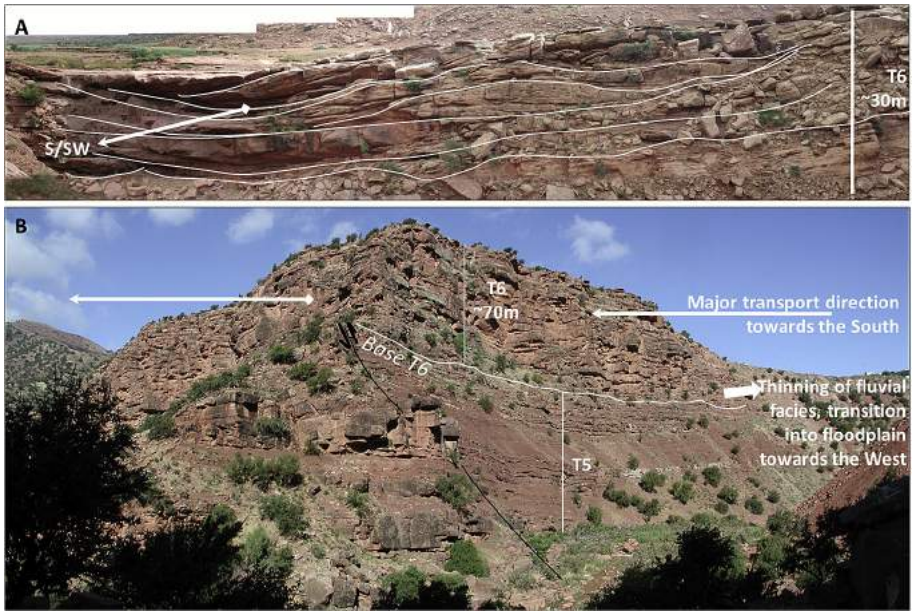

Fig. 15. Late fluvial phase Argana Valley. **15A** The Amzri section (locality 3) exposes T6 along a roughly E-W trending ridge. White lines highlight the internal fluvial architectural elements of a major river system draining towards the S, SW. **15B** 3D view along a modern river bend in the southern Argana Valley close to the Anglou Dam (locality 4) shows an approximately 70 m thick stacked fluvial unit, composed of amalgamated fine grained sandstone sheets. The fluvial package is thinning towards the W, and exhibits transition into distal floodplain fines in this direction. The main flow direction is towards the S. The system shows a highly aggradational pattern (see also Fig. 17B).

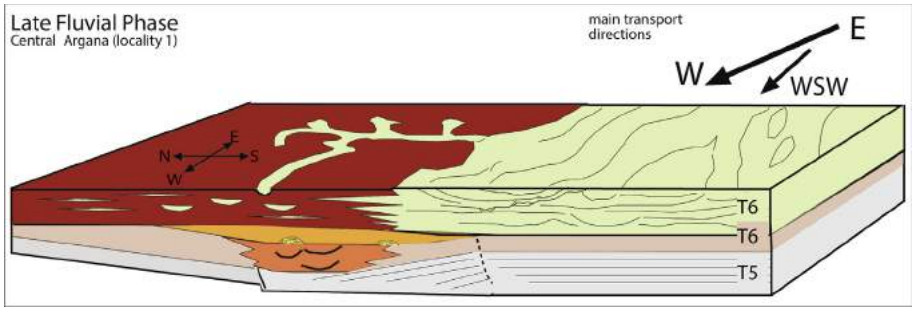

Fig. 16. Simplified depositional model for the late fluvial (perennial) phase (locality 1). Transport direction of fine grained, sand dominated fluvial sandstones is dominantly from East to West (WSW), and extensive floodplain fines to the North. In contrast to the early fluvial phase, the deposits are much cleaner, contain little to no extraformational clasts, and exhibit large (up to 2 m) bedforms of stacked fluvial dunes and bars. The fluvial system is laterally not confined as observed for the early phase.

8.4. Regional climate

The climate-driven overprint on sedimentation in the two studied basins is considered a major driver for sedimentary architectures, while higher-order tectonically induced changes in basin morphology and subsidence rates are assumed to have led to the sequence-scale basin fill. Sediments in both study areas were recognised to be strongly overprinted by the local climate and the climatic regime in the catchment-area (Hofmann et al., 2000; Mader and Redfern, 2011; this study). Sedimentological evidence from the Argana Valley suggest a cyclical evolution from: (a) a dominance of arid climatic conditions with subordinate cyclical humid pulses, resulting in the deposition of stacked ephemeral channel deposits, and a documented direct effect on local groundwater tables affecting deposition-preservation of aeolianites within the fluvial sequences; (b) an increase in humidity (discharge) inferred from a change in fluvial architecture to perennial flow, with deeply incising channels reflecting an amplified climatic signal; (c) a return to aridity with full aeolian conditions and minor humid pulses towards the top of T6. In the Essaouira Basin, an analogous climatic evolution with (a) ephemeral braided river deposits followed by abandonment of the system shifting into a wet aeolian sandflat environment, is interpreted to highlight prevailing arid conditions with sub-ordinate humid pulses; (b) the onset of perennial fluvial deposits with extensive floodplain fines and subordinate cyclical aridity expressed by calcrete deposits, documents a pronounced shift related to increased discharge and prominent humidity, most likely in the catchment area; (c) playa environment with extensive, highly mottled mudstones and predominately arid overprint record a return to overall aridity.

An intriguing aspect when comparing the Upper Triassic Essaouira with the Argana sequence is the observed well-defined shift from pronounced aridity to fluvial sedimentation with a prominent perennial character and a subsequent return to arid conditions. Moreover, the fluvial deposits exhibit sedimentary characteristics of long-lived, extensive perennial systems, atypical for the overall arid Triassic period. In the Essaouira Basin, the perennial deposits are for example associated with organic-rich shales and coaly interbeds, while in Argana the perennial fluvial

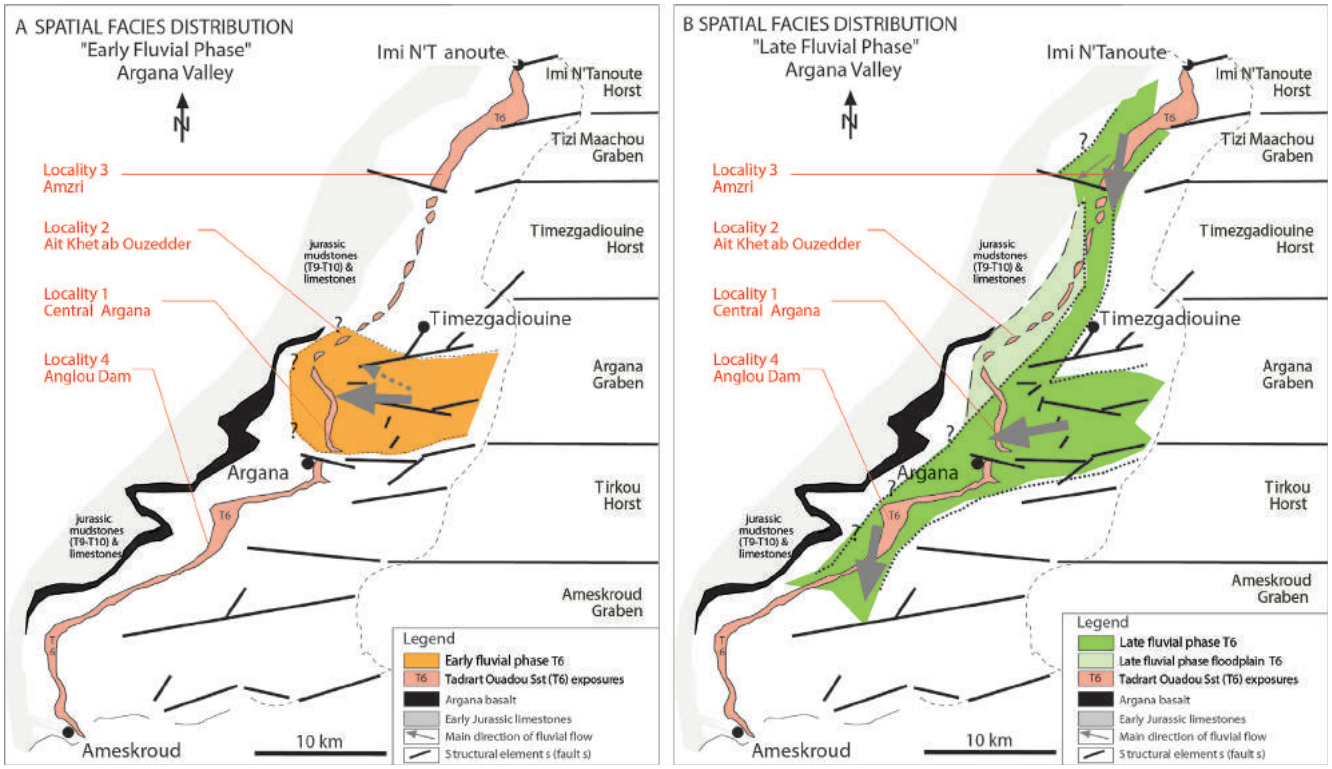

Fig. 17. Spatial sediment distribution of the early (**17A**) and late fluvial phases (**17B**) recognised for T6 in the Argana Valley. The distribution pattern is superimposed on the structural framework of Tixeront (1973). **17A** The limited extend of the early fluvial phase to the centre of the valley is highlighted, with a clear pinch-out mapped towards the S, N and NW. **17B** The spatial distribution of the late fluvial phase, with large, possibly longer-lived rivers extend throughout the entire valley exposures. Only in one locality (2) a dominance of aeolian deposits and only minor distal fluvial intercalations (away from main fairway) was recognised, why for this locality a fluvial margin position was postulated. The dominant transport direction of fluvial flow in locality 3 and 4 are towards the S (SW), whereas locality 1 exhibits an E-W (E-WSW) transport direction. Based on this facies distribution a roughly N-S running channel belt with extensive floodplain deposition, and a fluvial tributary systems from the E is postulated (green). Particularly for the N to S running channel belt, the hinterland source is more speculative and both the Anti Atlas, but also contribution from the Massie Ancien could be anticipated. (For interpretation of the references to colour in this figure legend, the reader is referred to the web version of this article.)

channels incise deeply into underlying strata, reflecting large river systems with exaggerate flow. This stands in direct contrast to the Triassic climate which is generally characterised by a "hot house" world with temperate warm conditions throughout (Kutzbach and Gallimore, 1989; Dubiel et al., 1991; Robinson, 1973; Parrish, 1994). Various climate models have in addition acknowledged the existence of extreme climatic regimes during the Triassic, and a dominance of strong monsoonal circulation patterns has been recognised (e.g. Kutzbach and Gallimore, 1989; Crowley et al., 1989, 1992; Dubiel et al., 1991; Parrish, 1994; Parrish and Curtis, 1982; Wang, 2009). Analogous to the modern monsoons, the Pangaean monsoonal circulations are thought to have occurred due to the sensible heating of the vast Pangaean continent, the symmetry across the equator during the Triassic enhancing cross-equatorial thermal contrast and the existence of the warm Tethyan seaway in-between maximising the pressure contrast (Young, 1987; Parrish, 1994; Kutzbach, 1994) (Fig. 18). Monsoonal circulation patterns can successfully be tested in the rock record (e.g. Nanson and Croke, 1992; Nanson et al., 1998; Radis et al., 2004; Sugai, 1993; Blum and Valastro, 1994; Holbrook, 2001; Gibling et al., 2005), and have been hinted at in studies of over-and underlying strata of the Argana Valley (Olsen et al., 2000; Hofmann et al., 2000). The strong seasonality, paleosols (calcretes) or coaly layers observed in the studied sections, further proposees a direct relationship to Pangean monsoonal patterns. On a regional scale, recent publications suggest particularly the Late Triassic was interrupted by a series of regionally significant humid events (e.g. Preto et al., 2010), the most prominent being the "Carnian pluvial event" (Simms and Ruffell, 1989, 1990; Simms et al., 1995; Parrish, 1994; Colombi and Parrish, 2008; Preto et al., 2010; Arche and Lopez-Gomez (2014)). The strong humid pulses preserved in the sedimentological record of Carnian to Norian strata in the Argana and Essaouira Basins could suggested that these pluvial events also impacted the SW Moroccan basins. Arche and Lopez-Gomez (2014) had already suggested that the Argana Basin fell within the regional trend of the Carnian pluvial event, and this study implies an even more regional extent to Essaouira. Similar to basins studied in Arche and Lopez-Gomez (2014) regional approach, the Essaouira sequence exhibits a shift to arid condition sedimentation patterns following the amplified humidity. In contrast to Arche and Lopez-Gomez (2014) however, the Tethyan transgression is not assumed to have reached as far west as Essaouira during the Carnian inferred from the lack of clear marine indicators from this core study (Fig. 18). Preto et al. (2010) summarised additional Upper Triassic humid events during the Norian, which have recently been documented along the northernmost extents of the Pangaen equatorial regions in the Central North Sea Basin (e.g. McKie, 2014). In view of the sparse age dating from Eassaouira it could be speculated, that there is a link to a later Norian humid event instead. Nevertheless, results from both Moroccan basins aid in redefining the paleogeographic and paleoclimatic setting along the south-eastern extends of the Tethyan margin (Fig. 18), placing them within the realm of mega-monsoonal oscillations during the Upper Triassic, and providing further evidence for the impact of regional pluvial events on the stratigraphy of SW Morocco. In terms of the direct effect of monsoonal oscillation patterns, general circulation models (GCMs)

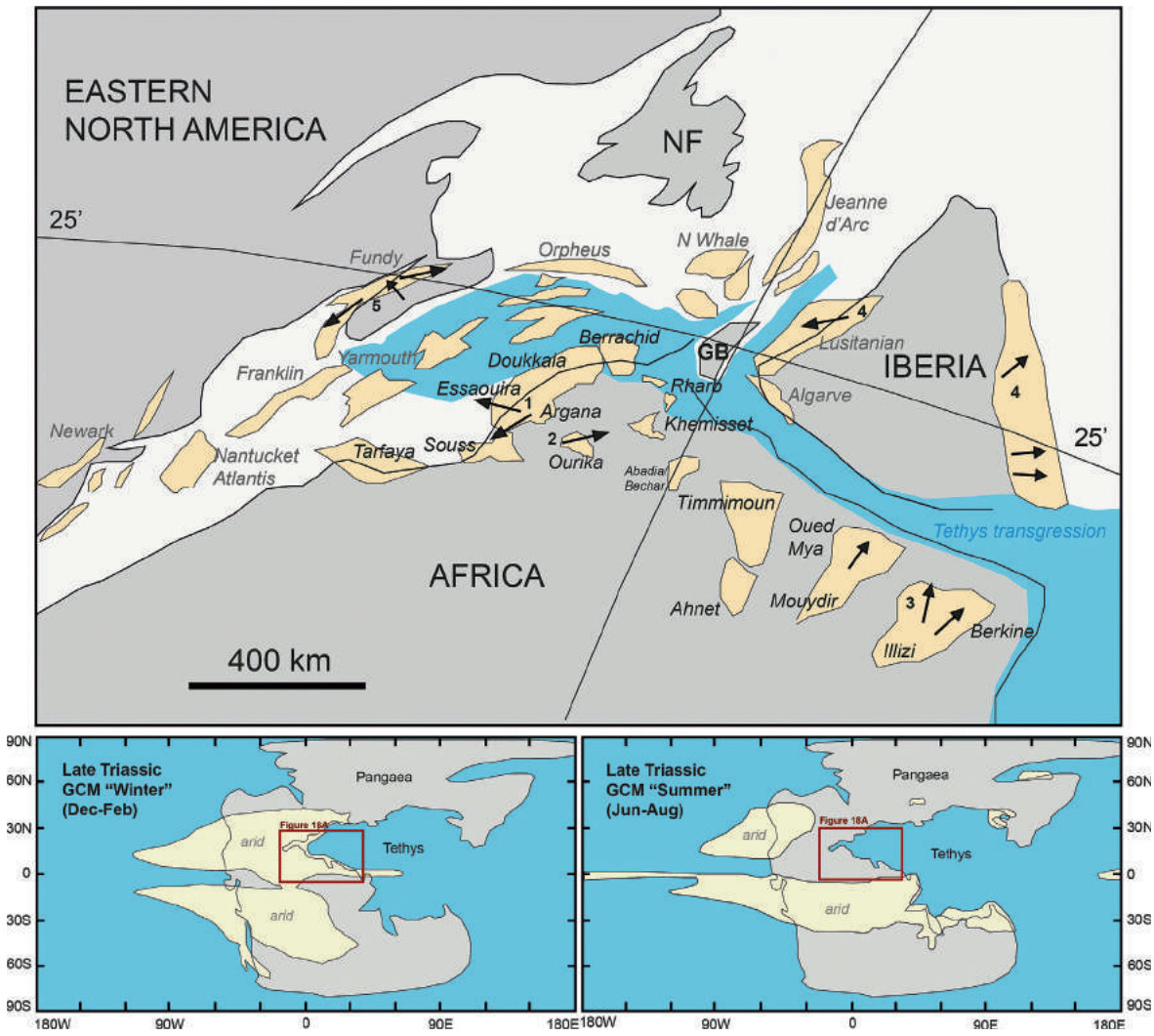

Fig. 18. Summarises regional aspects of Upper Triassic sedimentation patterns and the regional distribution of prevalent dry climates, modelled for Upper Triassic times (Sellwood and Valdes, 2006). **A** Regional location map of Triassic basins situated around 25′ N on the Pangaean continent within the main corridor of mega-monsoonal oscillations (*sensu* Kutzback and Gallimore, 1989) (map modified after Turner et al., 2001; Sahabi et al., 2004; Turner and Sherif, 2007; Arche and Lopez-Gomez (2014); Leleu et al., 2016). The black arrows highlight major transport directions of Upper Triassic alluvial/fluvial sediments investigated during this study, as well as from additional literature data (**1** this study; Mader and Redfern, 2011; **2** Fabuel-Perez et al., 2009a,b; **3** Turner et al., 2001 **4** Arche and Lopez-Gomez (2014); **5** Mader, 2005; Hubert and Forlenza, 1988). Super-imposed is the extend of the Tethyan ocean towards the W during Carnian times (after Arche and Lopez-Gomez, 2014 with edits for the central Essaouira Basin). For the Essaouira basin the paleogeographic model was modified from the original as a result of this study, which suggests major marine incursions to be later than Carnian, possibly as late as Earliest Liassic. **B & C** General circulation models (GCMs) for the Upper Triassic (simplified after Sellwood and Valdes, 2006) . **B** shows the modelled simulation of mean seasonal precipitation for the northern hemisphere "winter" season (December- January–February) of the Upper Triassic Pangaean continent. The red box positions the AOI and its surrounding basins in a zone of pronounced aridity (<0.5 mm/day rainfall), while during the summer months (June-July-August) mean seasonal precipitation is modelled to be < 8 mm/day in the equatorial top low latitudes surrounding the eastern Tethys (summerwet, tropical). The annual shift between these climatic extremes results in extensive evaporite and calcrete deposition in the Tethyan region (Scotese, 2000). While Argana exhibits a more intra mountainous year-round arid climate, possibly in a rain-shadow position, evidence from the Meskala Field of calcrete deposits as well as coaly interbeds points towards direct influence of monsoonal-oscillations with an overall hot and predominantly arid climate interspersed with short wet seasons. (For interpretation of the references to colour in this figure legend, the reader is referred to the web version of this article.)

for Pangaea during Upper Triassic times (Sellwood and Valdes, 2006) give rise to multiple assumption as to when strong rainfall could have affected the AOI (figures 18A,C): during the winter monsoon, as predicted for Arabia and NE Africa (Fig. 18B), or during the tropical summer monsoon (Fig. 18C). The predominantly E to W wind directions preserved in aeolianites of T6 in the Argana Valley led Mader and Redfern (2011) to believe that the climatic regime during the arid phases reflects the Pangaean winter, while humid pulses are driven by the Pangaean summer monsoon, however also point out the possibility of a rainshadow position. Whether maximum rainfall affected the AOI during Pangaean summers, or whether the Pangaean winter monsoon modelled for Arabia and NE Africa reaches as far as SW Morocco remains speculative, however provides clear evidence for the eastern extends of monsoonal oscillations affecting the SW Moroccan basins in general.

9. Conclusions

Depositional model Essaouira Basin (Meskala Field)

Detailed core analysis from the main reservoir unit in the Meskala Field (central Essaouira Basin) has led to a defined suite of facies associations, which merit a new facies model for the Upper Triassic deposits. Four facies associations were defined and interpreted to represent a progressive evolution from ephemeral fluvial deposits characterised by episodic discharge in a shallow braided

river system, evolving into a wet sandflat environment during a phase of pronounced aridity. Above a clear bounding surface, a rapid change in depositional environment from sheet-like ephemeral flow to metre-scale fluvial sandstone packages with very fine-grained channel deposits and abundant, thick floodplain fines follows. Several fining-upward sequences were documented, and a fluvial perennial river setting is proposed. Subsequently, the fluvial deposits become increasingly overprinted by transgressive phases of an adjacent lacustrine or playa lake shifting shoreline. The environment of deposition changes into a delta setting with distributary mouthbars and abundant inter-pond areas on the delta-top. The sandstones change from clearly defined fluvial channel deposits to dominantly ripple cross-stratified sandstones with abundant organic-rich intercalations and paleosols preserved on the floodplain. Water availability and more perennial conditions were inferred. Towards the end of this transgressive phase, the overall input of sandstones decreases considerably and an extensive playa environment returning to oxidising conditions in an arid climate is proposed.

Regional sediment distribution patterns SW Morocco

A comparison is made between the studied deposits in the Essaouira Basin and time-equivalent sections of Carnian to Norian age in the Argana Valley. The key question, whether sediments exposed in the Argana Valley were directly linked to the Essaouira Basin, affording a direct sediment source for the prolific Upper Triassic reservoirs in the Meskala Field is addressed. Although a proximal to distal facies relationship between the Argana Valley and Essaouira Basin is superficially apparent, SE to NW directed fluvial flow was only subordinately recognised in the Argana Valley questioning this direct source to sink relationship. Sedimentological data from the sandstone dominated facies in the Argana Valley indicate a dominantly W to SW to S paleoflow instead, which on a regional scale supports increased accommodation creation to the S/SW. Regional sedimentary evidence further suggests that sediment storage during the Carnian to Norian is likely to be in the southern Argana Valley or southern Souss Basins, which gradually filled during the Upper Triassic, masking the previous inherent structural grain of initial half-grabens (Hofmann et al., 2000; Mader and Redfern, 2011; Baudon et al., 2012). No evidence for continuous, extensive NW flowing fluvial flow which would have been representative of a direct sediment fairway to the central Essaouira Basin was recognised, hence a more local provenance for the Meskala reservoirs is anticipated.

Paleo-climatic implications

Pronounced, possibly short but intensive wet seasons in an otherwise dominantly hot, arid climatic setting were documented in both studied localities. A link is made to regionally extensive Upper Triassic pluvial events such as the well document “Carnian pluvial event”. Results from this study aid in breaching the gap for paleogeographic and paleo-climatic reconstructions of the eastern Atlantic margin and the extent of Late Triassic Tethys transgressions.

Acknowledgments

This work is part of a PhD thesis completed at the University of Manchester, UK. The North Africa Research Group and sponsoring companies provided the financial support necessary to carry out field work. ONHYM kindly provided access to the sub-surface data sets and allowed publication of the data. The reviewers S. Leleu (Université of Bordeaux Montaigne) and S. Jones (Durham University) provided valuable comments that improved the initial manuscript considerably.

References

Ait Chayeb, E.H., Youbi, N., El-Boukhari, A., Bouabdelli, M., Amrhar, M., 1998. Permian–mesozoic volcanism of the Argana Basin (western high Atlas, Morocco); intraplate magmatism associated with the opening of the Central Atlantic. J. Afr. Earth Sci. 26, 499–519.
Alonso-Zarza, A.M., 2003. Palaeoenvironmental significance of palustrine carbonates and calcretes in the geological record. Earth Sci. Rev. 60, 261–298.
Anderson, M.P., Aiken, J.S., Webb, E.K., Mickelson, D.M., 1999. Sedimentology and hydrology of two braided stream systems. Sediment. Geol. 129, 187–200.
Arche, A., 2007. Some precisions on the use of the term playa in the geologic literature. J. Iber. Geol. 24, 5–10.
Arche, A., Lopez-Gomez, J., 2014. The Carnian pluvial event in western Europe: new data from Iberia and correlation with the Western Neotethys and Eastern North America – NW Africa regions. Earth Sci. Rev. 128, 196–231.
Audley-Charles, M.F., 1970. Triassic palaeogeography of the British Isles. Q. J. Geol. Soc. Lond. 126, 49–89.
Baudon, C., Redfern, J., Driessche, Van Den, 2012. Permo-Triassic structural evolution of the Argana Valley, impact of the Atlantic rifting in the high Atlas, Morocco. J. Afr. Earth Sci. 65, 91–104.
Beauchamp, J., 1988. Triassic sedimentation and rifting in the high Atlas (Morocco). In: Manspeizer, W. (Ed.), Triassic-Jurassic Rifting, Developments in Geotectonics, vol. 22, pp. 477–497.
Blum, M.D., Törnqvist, T.E., 2000. Fluvial responses to climate and sea-level change: a review and look forward. Sedimentology 47, 2–48.
Blum, M.D., Valastro, S.J., 1994. Late Quaternary sedimentation, lower Colorado River, Gulf Coastal plain of Texas. Geol. Soc. Am. Bull. 106 (8), 1002–1016.
Bouatmani, R., Ahmamou, M., El Ouarghioui, A., Medina, F., El Mourabit, A., Daoudi, L., 2004. Les environnements de dépôt des formations triasiques de la région de Meskala (bassin d'Essaouira, Maroc): apport de l'analyse des diagraphies et des carottes. Bull. Inst. Sci. Rabat, Sect. Sci. Terre 26, 49–67.
Bridge, J.S., 1993. The interaction between channel geometry, water flow, sediment transport and deposition in braided rivers. In: Best, J.L., Bristow, C.S. (Eds.), Braided Rivers, Geological Society of London, Special Publications, 75, pp. 13–71.
Bridge, J.S., 2003. Rivers and Floodplains. Blackwell, Oxford.
Bridge, J.S., 2006. Fluvial facies models: recent developments. In: Posamentier, W., Walker, R.G. (Eds.), Facies Models Revisited, vol. 84. SEPM Special Publication, pp. 85–170.
Bristow, C.S., Skelly, R.L., Ethridge, F.G., 1999. Crevasse splays from the rapidly aggrading, sandbed, braided Niobrara River, Nebraska: effect of base-level rise. Sedimentology 46, 1029–1047.
Broughton, P., Trépanier, P., 1993. Hydrocarbon generation in the Essaouira Basin of western Morocco. AAPG Bull. 77 (6), 999–1015.
Brown, R.H., 1980. Triassic rocks of the Argana Valley, southern Morocco, and their regional structural implications. AAPG Bull. 64 (7), 988–1003.
Cain, N.P., Mountney, N.P., 2009. Spatial and temporal evolution of a terminal fan system: the Permian Organ Rock Formation, SE Utah, USA. Sedimentology 56, 1774–1800.
Colombera, L., Mountney, N.P., McCaffrey, W.D., 2015. A meta-study of relationships between fluvial channel-body stacking pattern and aggradation rate: implications for sequence stratigraphy. Geology 43, 283–286.
Colombi, C.E., Parrish, J.T., 2008. Late Triassic environmental evolution in Southwestern Pangae: plant taphonomy of the Ischigualasto formation. Palaios 23, 778–795.
Courel, L., Ait Salem, H., Benaouiss, N., Et-Touhami, M., Fekirine, B., Oujidi, M., Soussi, M., Tourani, A., 2003. Mid-Triassic to early Jurassic clastic/evaporitic deposits over the Maghreb platform. Palaeogeography, Palaeoclimatology. Palaeoecology 196/1, 157–176.
Crowley, T.J., Hyde, W.T., Short, D.A., 1989. Seasonal cycle variations on the supercontinent of Pangaea: implications for Early Permian vertebrate extinctions. Geology 17, 457–460.
Crowley, T.J., Kim, K.Y., Mengel, J.G., Short, D.A., 1992. Modelling 100,000-year climate fluctuations in pre-Pleistocene time series. Science 255 (5045), 705–707.
Deenen, M., Langreis, C., Krijgsman, W., ElHachimi, W., Chellai, E.H., 2010. Palaeomagnetic results from Upper Triassic red-beds and CAMP lavas of the Argana Basin, Morocco. In: Van Hinsbergen, D.J.J., Buiter, S.J.H., Torsvik, T.H., Gaina, C., Webb, S.J. (Eds.), The Formation and Evolution of Africa: a Synopsis of 3.8 Ga of Earth History, vol. 357. Geological Society, London, Special Publications, pp. 195–209.
Dubiel, R.F., Parrish, J.T., Parrish, M., Good, S.C., 1991. The Pangaean Megamonsoon - evidence from the Upper Triassic Chinle formation, Colorado plateau. Palaios 6, 347–370.
Duffaut, M.F., Brun, L., Plauchut, B., 1966. Notes mém'Serv. Géol. Maroc. 85, 129–137.
Dutuit, J.M., 1976. Introduction à l'étude paléontologique du Trias continental marocain. Description des premièrs Stégocéphales recueillis dans le couloir d'Argana. Mém. Mus. Natn. Hist. Nat. Paris, C 36, 253.
Dutuit, J.M., 1977. Palaeorhinus magnoculus, phytosaure du Trias supérieur de l'Atlas Marocain. Géologie Méditerranéenne 4, 225–238.

Dutuit, J.M., 1988. Diplocaulus minimus n. ps. (Amphibia; Nectridea), Lepospondyle de la formation d'Argana, dans l'Atlas occidental marocain. C.R. Acad. Sci. Paris, II 307, 851–854.
El Hachimi, H., Youbi, N., Madeira, J., Bensalah, M.K., Martins, L., Mata, J., Medina, F., Bertrand, H., Marzoli, A., Munhá, J., Bellieni, J., Mahmoudi, A., Ben Abbou, M., Assafar, H., 2011. Morphology, internal architecture, and emplacement mechanisms of lava flows from the Central Atlantic Magmatic Province (CAMP) of Argana basin (Morocco). In: Van Hinsbergen, D.J.J., Buiter, S., Torsvik, T.H., Gaina, C., Webb, S. (Eds.), The Formation and Evolution of Africa : a Synopsis of 3.8 Ga of Earth History, the Geological Society of London, Special Publication, 357, pp. 167–193.
Fabuel-Pérez, I., Hodgetts, D., Redfern, J., 2009a. A new approach for outcrop characterization and geostatistical analysis of a low-sinuosity fluvial-dominated succession using digital outcropmodels: Upper Triassic Oukaimeden Sandstone Formation, High Atlas, Morocco. AAPG Bull. 93, 795–827.
Fabuel-Pérez, I., Redfern, J., Hodgetts, D., 2009b. Sedimentology of an intra-montane rift-controlled fluvial-dominated succession: the Upper Triassic Oukaimeden Sandstone formation, Central high Atlas, Morocco. Sediment. Geol. 218, 103–140.
Fiechtner, L., Friedrichsen, H., Hammerschmidt, K., 1992. Geochemistry and geochronology of early Mesozoic tholeiites from Central Morocco. Int. J. Earth Sci. 81 (1), 45–62.
Fisher, J.A., Nichols, G.J., Waltham, D.A., 2008. Unconfined flow deposits in distal sectors of fluvial distributary systems: examples from the Miocene Luna and Huesca Systems, northern Spain. Sediment. Geol. 195 (2008), 55–77.
Gibling, M.R., Tandon, S.K., Sinha, R., Jain, M., 2005. Discontinuity-bounded alluvial sequences of the southern Gangetic plains, India: aggradation and degradation in response to monsoonal strength. J. Sediment. Res. 75, 369–385.
Glennie, K.W., 1970. Desert Sedimentary Environments. Elsvier, Amsterdam.
Gradstein, F., Ogg, J., Schmitz, M., Ogg, G., 2012. The Geologic Timescale, 2 vol.. Elsvier.
Hafid, M., 2000. Triassic - early Jurassic extensional systems and their Tertiary inversion, Essaouira Basin (Marocco). Mar. Petrol. Geol. 17, 409–429.
Hafid, M., Ait Salem, A., Bally, A.W., 2000. The western termination of the Jebilet-high Atlas system (offshore Essaouira Basin, Morocco). Mar. Petrol. Geol. 17, 431–443.
Hinz, K., Dostmann, H., Fritsch, J., 1981. The continental margin of Morocco: seismic sequences, structural elements and geological development. In: Von Rad, U., Hinz, K., Sarnthein, M., Seibold, E. (Eds.), Geology of the Northwest African Margin.
Hminna, A., Voigt, S., Saber, H., Schneider, J.W., Hmich, D., 2012. On a moderately diverse continental ichnofauna from the Permian Ikakern Formation (Argana Basin, Western High Atlas, Morocco). J. Afr. Earth Sci. 68, 15–23.
Hofmann, A., Tourani, A., Gaupp, R., 2000. Cyclicity of Triassic to Lower Jurassic continental red beds of the Argana Valley, Morocco: implications for palaeoclimate and basin evolution. Palaeogeogr. Palaeoclimatol. Palaeoecol. 161, 226–266.
Holbrook, J., 2001. Origin, genetic interrelationships, and stratigraphy over the continuum of fluvial channel-form bounding surfaces: an illustration from middle Cretaceous strata, southeastern Colorado. Sediment. Geol. 144, 179–222.
Howell, J., Mountney, N., 1997. Climatic cyclicity and accommodation space in arid to semi-arid depositional systems: an example from the Rotliegend Group of the UK southern North Sea. In: Ziegler, K., Turner, P., Daines, S.R. (Eds.), Petroleum Geology of the Southern North Sea: Future Potential, Geological Society London Special Publications, 123, pp. 63–86.
Hubert, J.F., Forlenza, M.F., 1988. Sedimentology of braided-river deposits in Upper Triassic Wolfville redbeds, southern shore of Cobequid Bay (sic), Nova Scotia, Canada. In: Manspreizer, W. (Ed.), Triassic-Jurassic Rifting: Continental Breakup and the Origin of Atlantic Ocean and Passive Margins. Elsevier, Amsterdam, Netherlands, pp. 231–247.
Hunt, A.P., Lucas, S.G., 1991. The Palaeorhinus Biochron and the correlation of the non-marine upper Triassic of Pangaea. Palaeontology 34, 487–501.
Jalil, N.-E., 1999. Continental Permian and Triassic vertebrate localities from Algeria and Morocco and their stratigraphical correlations. J. Afr. Earth Sci. 29 (1), 219–226.
Jalil, N.-E., Dutuit, J.-M., 1996. Permian captorhinid reptiles from the Argana formation, Morocco. Palaeontology 39 (4), 907–918.
Jalil, N.E., Janvier, P., 2005. Les pareiasaures (Amniota, Parareptilia) du Permien supérieur du Bassin d'Argana, Maroc. Geodiversitas 27, 35–132.
Jalil, N.E., Peyer, K., 2007. A new rauisuchian (Archosauria, Suchia) from the Upper Triassic of the Argana Basin, Morocco. Palaeontology 50 (2), 417–430.
Jalil, N.-E., Janvier, P., Steyer, J.-S., 2009. A new cyclotosaurid (Amphibia, Temnospondyli) from the Triassic of Argana Basin (High Atlas mountains, Morocco), biostratigraphic implications. In: 1st Int. Congr. N. African Vertebr. Palaeontol, pp. 36–37. Abstracts (2009).
Jansa, L.F., Wiedmann, J., 1980. Mesozoic-Cenozoic development of the E North American and Northwest African continental margins: a comparison. In: Von Rad, U., Hinz, K., Sarnthein, M., Seibold, E. (Eds.), Geology of the Northwest African Margin.
Jones, D.F., 1975. Stratigraphy, environments of deposition, petrology, age, and provenance of the basal red beds of the Argana Valley, Western High Atlas Mountains, Morocco. New Mexico Institute of Mining and Technology, Socorro, New Mexico, p. 144.
Jopling, A.V., Walker, R., 1968. Morphology and origin of ripple-drift cross-lamination, with examples from the Pleistocene of Massachusetts. J. Sediment. Petrol. 38, 971–998.
Khalaf, I.F., 2007. Occurrence and genesis of calcrete and dolocrete in the Mio-Pleistocene fluviatile sequence in Kuweit, northeast Arabian Peninsula. Sediment. Geol. 199, 129–139.
Klein, H., Voigt, S., Hminna, A., Saber, H., Schneider, J., Hmich, D., 2010. Early Triassic Archosaur-dominated footprint assemblage from the Argana Basin (Western High Atlas, Morocco). Ichnos 17, 215–227.
Klein, H., Voigt, S., Hminna, A., Saber, H., Schneider, J., Fischer, J., Brosig, A., 2011. First occurrence of a Middle Triassic tetrapod ichnofauna from the Argana Basin (Western High Atlas, Morocco). Palaeogeogr. Palaeoclimatol. Palaeoecol. 307, 218–231.
Knight, K.B., Nomade, S., Renne, P.R., Marzoli, A., Betrand, H., Youbi, N., 2004. The Central Atlantic magmatic province at the Triassic–Jurassic boundary: paleomagnetic and 40Ar/30Ar evidence from Morocco for brief, episodic volcanism. Earth Planet. Sci. Lett. 22, 143–160.
Kocurek, G., 1988. Late Palaeozoic and Mesozoic eolian deposits of the western interior of the United States. Sediment. Geol. 56, 3–125. Special Issue.
Kocurek, G., Nielson, J., 1986. Conditions favourable for the formation of warm-climate aeolian sand sheets. Sedimentology 33, 795–816.
Kumar, R., Ghosh, S.K., Satish, J.S., 1999. Evolution of a Neogene fluvial system in a Himalayan foreland basin, India. In: Macfarlane, A., Sorkhabi, R.B., Quade, J. (Eds.), Himalaya and Tibet Mountain Roots to Mountain Tops, Geological Society of America, Special Papers, 328, pp. 239–256.
Kutzbach, J.E., 1994. Idealized Pangaean climates: Sensitivity to orbital change. In: Klein, G.D. (Ed.), Pangaea: Palaeoclimate, Tectonics, and Sedimentation during Accretion, Zenith, and Brea-kup of a Super-continent, vol. 288. Geological Society of America, Boulder, CO, pp. 41–55.
Kutzbach, J.E., Gallimore, R.G., 1989. Pangaean climates: Megamonsoons of the Megacontinent. J. Geophys. Res. 94 (D3), 3341–3357.
Laville, E., Petit, J.-P., 1984. Role of syn-sedimentary strike-slip faults in the formation of Moroccan Triassic basin. Geology 12, 424–427.
Leleu, S., Hartley, A.J., 2010. Controls on the stratigraphic development of the Triassic Fundy basin, Nova Scotia: implications for the teconostratigraphic evolution of Triassic Atlantic rift basins. J. Geol. Soc. Lond. 167, 437–454.
Leleu, S., Hartley, A.J., Van Oosterhout, C., Kennan, L., Ruckwied, K., Gerdes, K., 2016. Structural, stratigraphic and sedimentological characterisation of a wide rift system: The Triassic rift system of the Central Atlantic Domain. Earth Sci. Rev. 158, 89–124.
LeRoy, P., Pique, A., 2001. Triassic-jurassic Western Moroccan synrift basins in relation to the Central Atlantic opening. Mar. Geol. 172, 359–381.
LeRoy, P., LeGall, B., Ait Rahim, L., Morabet, A.M., Demnati, A., 1997. Les basins côtiers triasico-liasiques du Maroc occidental et la diachronie du rifting intra-continental de L'Atlantique central. Bull. la Société géologique Fr. 168, 637–648.
Lucas, S.G., 1998. Global Triassic tetrapod biostratigraphy and biochronology. Palaeogeogr. Palaeoclimatol. Palaeoecol. 143, 347–384.
Mader, N.K., 2005. Sedimentology and Sediment Distribution of Upper Triassic Fluvio-aeolian Reservoirs on a Regional Scale (Central Algeria, SW Morocco, NE Canada): an Integrated Approach Unravelling the Influence of Climate versus Tectonics on Reservoir Architecture. Unpublished PhD thesis. Manchester University, UK.
Mader, N.K., Redfern, J., 2011. A sedimentological model for the continental upper Triassic Tadrart Ouadou Sandstone member : recording an interplay of climate and tectonics (Argana Valley; SW Morocco). Sedimentology 58 (5), 1247–1282.
Manspeizer, W., 1982. Triassic-jurassic Basins and Climate of the Atlantic passive margins. Geol. Rundsch. 71 (3), 895–917.
Manspeizer, W., 1988. A stratigraphic record from Morocco and North America of rifting, drifting and Tethyan transgression of the Central proto-Atlantic. J. Afr. Earth Sci. 7 (2), 369–373.
Manspeizer, W., 1994. The breakup of Pangaea and its impact on climate: consequences of Variscan-Alleghanianide orogenic collapse. In: Klein (Ed.), Pangaea: Palaeoclimate, Tectonics and Sedimentation during Accreation, Zenith and Breakup of a Supercontinent. Geol. Soc. Am. Spec. Pap., vol. 288, pp. 169–185.
Manspeizer, W., Puffer, J.H., Cousminer, H.L., 1978. Separation of Morocco and E North America: a Triassic-Jurassic stratigraphic record. Geol. Soc. Am. Bull. 89, 901–920.
Mariott, S.B., Alexander, J. (Eds.), 1999. Floodplains: Interdisciplinary Approaches. Geol. Soc. London, Spec. Pub., 28, pp. 271–281.
Marzoli, A., Renne, P.R., Piccirillo, E.M., Ernesto, M., Belliene, G., De Min, A., 1999. Extensive 200-million-year-old Continental Flood Basalts of the Central Atlantic Magmatic Province. Science 23 April 1999, 284(5414), pp. 616–618.
Marzoli, A., Bertrand, H., Knight, K.B., Cirilli, S., Buratti, N., Vérati, C., Nomade, S., Renne, P.R., Youbi, N., Martini, R., Allenbach, K., Neuwerth, R., Rapaille, C., Zaninetti, L., Bellieni, G., 2004. Synchrony of the Central Atlantic magmatic province and the Triassic-Jurassic boundary climatic and biotic crisis. Geology 32, 973–976.
Matthews, M.D., Perlmutter, M.A., 1994. Global cyclostratigraphy: an application to the Eocene Green River Basin. In: De Boer, P.L., Smith, D.G. (Eds.), Orbital Forcing and Cyclical Sequences. Blackwell Scientific Publications, Oxford.
Mattis, A.F., 1977. Nonmarine Triassic sedimentation, central high Atlas mountains, Morocco. J. Sediment. Petrol. 47 (1), 107–119.
McHone, G., 2000. Non-plume magmatism and rifting during the opening of the central Atlantic Ocean. Tetconophysics 316, 287–296.
McKie, 2014. Climatic and tectonic controls on Triassic dryland terminal fluvial system architecture, central North Sea. Int. Assoc. Sedimentol. Spec. Publ. 46, 19–58.

Medici, G., Boulesteix, Mountney, N.P., West, L.J., Odling, 2015. Paleoenvironment of braided fluvial systems in different tectonic realms of the Triassic Sheerwood Sandstone Group, UK. Sediment Geol. 329, 188–210.
Medina, F., 1988. Tilted-blocks pattern, paleostress orientation and amount of extension, related to triassic early rifting of the central Atlantic in the Amzri area (Argana basin, Morocco). Tectonophysics 148 (3–4), 229–233.
Medina, F., 1991. Superimposed extensional tectonics in the Argana Triassic formations (Morocco), related to the early rifting of the central Atlantic. Geol. Mag. 128 (5), 525–536.
Medina, F., 1995. Syn- and postrift evolution of the El Jadida-Agadir basin (Morocco): constraints for the rifting models of the central Atlantic. Can. J. Earth Sci. 32, 1273–1291.
Miall, A.D., 1977. A review of the braided-river depositional model environment. Earth Sci. Rev. 13, 1–62.
Miall, A.D., 1996. The Geology of Fluvial Deposits. In: Sedimentary Facies, Basin Analysis and Petroleum Geology. Springer-Verlag, Heidelberg.
Miall, A.D., 2006. The Geology of Fluvial Deposits. In: Sedimentary Facies, Basin Analysis and Petroleum Geology. Springer, Berlin.
Morabet, A.M., Bouchta, R., Jabour, H., 1998. An overview of the petroleum systems of Morocco. In: MacGregor, D.S., Moody, R.T.J., Clark-Lowes, D.D. (Eds.), Petroleum Geology of North Africa, Geological Society London Special Publication, 132, pp. 283–296.
Nanson, G.C., Croke, J.C., 1992. A genetic classification of floodplains. Geomorphology 4, 459–486.
Nanson, G.C., Rust, B.R., Taylor, G., 1986. Coexistent mud braids and anastomosing channels in arid zone river: Cooper Creek, Central Australia. Geology 14, 175–178.
Nanson, G.C., Callen, R.A., Price, D.M., 1998. Hydroclimatic interpretation of Quaternary shorelines on South Australian playas. Palaeogeogr. Palaeoclimatol. Palaeoecol. 144, 281–305.
Newell, A.J., Tverdokhlebov, V.P., Benton, M.J., 1999. Interplay of tectonics and climate on a transverse fluvial system, Upper Permian, Southern Uralian foreland Basin, Russia. Sediment. Geol. 127, 11–29.
Nomade, S., Knight, K.B., Beutel, E., Renne, P.R., 2007. Chronology of the Central Atlantic magmatic province: implications for the Central Atlantic rifting processes and the Triassic–Jurassic biotic crisis. Palaeogeogr. Palaeoclimatol. Palaeoecol. 244, 326–344.
Olsen, P.E., Kent, D.V., Fowell, S.J., Schlische, R.W., Withjack, M.O., LeTourneau, P.M., 2000. Implications of a comparison of the stratigraphy and depositional environments of the Argana (Morocco) and Fundy (Nova Scotia, Canada) Permian-Jurassic basins. In: Oujidi, M., Et-Touhami, M. (Eds.), Le Permien et le Trias du Maroc: Acte de la Premiere Reunion du Groupe Marocain du Permien et du Trias, Oujda, pp. 165–183.
ONAREP (Office National de Recherches et d'Explorations Petrolieres, Morocco), 1995. Onshore Essaouira Basin: Exploration Prospects Morocco. ONAREP Report (1995), pp. 1–24.
Oujidi, M., Courel, L., Benaouiss, N., El Mostaine, M., El Touhami, M., Ouarhache, D., Sabaoui, A., Tourani, A.-I., 2000. Triassic series of Morocco: stratigraphy, paleogeography and structuring of the southwestern Peri-Tethyan Platform. An overview. In: Crasquin-Soleau, S., Barrier, E. (Eds.), Peri-tethys Memoir 5: New Data on Peri-tethyan Sedimentary Basins, Mem. Mus. Natn. Hist. nat., 182: 23–38. Paris.
Owens, P.M., Walling, D.E., Leeks, G.J.L., 1999. Deposition and storage of fine-grained sediment within the main channel system of the River Tweed, Scotland. Earth Surf. Process. Landforms 24, 1061–1076.
Parrish, J.T., 1994. Climate of the supercontinent Pangaea. J. Geol. 101, 215–233.
Parrish, J.T., Curtis, R.L., 1982. Atmospheric circulation, upwelling, and organic-rich rocks in the Mesozoic and Cenozoic eras. Palaeogeogr. Palaeoclimatol. Palaeoecol. 40, 31–66.
Piqué, A., Laville, E., 1996. The central Atlantic rifting: reactivation of Palaeozoic structures? J. Geodyn. 21, 235–255.
Piqué, A., Le Roy, P., Amrhar, M., 1998. Transtensive synsedimentary tectonics associated with ocean opening: the Essaouira-Agadir segment of the Moroccan Atlantic margin. J. Geol. Soc. Lond. 155, 913–928.
Platt, N.H., Keller, B., 1992. Distal alluvial deposits in a foreland basin setting—the Lower Freshwater (Miocene), Switzerland: sedimentology, architecture and palaeosols. Sedimentology 39 (1992), 545–565.
Preto, N., Kustatscher, E., Wignall, P.B., 2010. Triassic climates – state of the art and perspectives. Paleogeogr. Paleoclimatol. Palaeoecol. 290, 1–10.
Radis, D., Preusser, F., Matter, A., Mange, M., 2004. Eustatic and climatic controls on the development of the Wahiba Sand Sea, Sultanate Oman. Sedimentology 51, 1359–1385.
Reeves Jr., C.C., 1976. Caliche Origin, Classification, Morphology and Uses. Estacado Books, Lubbock.
Retallack, G.J., 1988. Field recognition of palaeosols. In: Geological Society of America Special Paper, 216, pp. 1–20.
Robinson, P.L., 1973. Paleoclimatology and continental drift. In: Tarling, D.H., Runcorn, S.K. (Eds.), Implications of Continental Drift to the Earth Sciences. Academic Press, London, pp. 449–476.
Sahabi, M., Aslanian, D., Olivet, J.L., 2004. Un nouoveasu point depart pour l'histore de l'Atlantique central. C.R. Geosci. 336, 1041–1052.
Schumm, S.A., 1968. Speculations concerning palaeohydrologic controls of terrestrial sedimentation. Geol. Soc. Am. Bull. 79, 1573–1588.
Schumm, S.A., 1993. River response to base-level changes: implications for sequence stratigraphy. J. Geol. 101, 279–294.
Scotese, C.R., 2000. Paleomap Project. http://www.scotese.com.
Sellwood, B.C., Valdes, P.J., 2006. Mesozoic climates: general circulation models and the rock record. Sediment. Geol. 190, 269–287.
Shanley, K.W., McCabe, P.J., 1994. Perspectives on the sequence stratigraphy of continental strata. Am. Assoc. Petrol. Geol. Bull. 78, 544–568.
Silmane, A., ElMostaine, M., 1997. Observations biostratigraphique au niveau des formations rouge de la séquence synrift dans le bassins de Doukkla et Essaouira. In: 1ère Réunion du Groupe marocain du Permien et du Trias, Oujda, Maroc, vol. 54. Faculté des Science, Université Mohammed I, Oujda.
Simms, M.J., Ruffell, A.H., 1989. Synchroneity of climatic change and extinctions in the Late Triassic. Geology 17, 265–268.
Simms, M.J., Ruffell, A.H., 1990. Climatic and biotic change in the late Triassic. J. Geol. Soc. Lond. 147, 321–327.
Simms, M.J., Ruffell, A.H., Johnson, L.A., 1995. Biotic and climatic changes in the Carnian (Tiassic) of Europe and adjacent areas. In: Fraser, N.C., Sues, H.-D. (Eds.), In the Shadow of the Dinosaurs: Early Mesozoic Tetrapods. Cambridge University Press, pp. 352–365.
Smoot, J.P., 1991. Sedimentary facies and depositional environments of early Mesozoic Newark Supergroup basins, eastern North America. Paleogeogr. Paleoclimatol., Palaeoecol. 84, 369–423.
Societe Cherifienne des Petroles, 1966. Le basin du sud-ouest marocain. In: Reyre, D. (Ed.), Sedimentary Basins of the African Coast. Assoc. Geol. Soc. Africains, Paris, pp. 5–12.
Stets, J., Wurster, P., 1981. Atlas and Atlantic-structural relations. In: Von Rad, U., Hinz, K., Sarnthein, M., Seibold, E. (Eds.), Geology of the Northwest African Margin, pp. 68–84.
Sugai, T., 1993. River terrace development by concurrent fluvial processes and climatic changes. Geomorphology 6, 243–252.
Tixeront, M., 1973. Lithostratigraphie et minéralisations cuprifères et uranifères stratiformes syngenetiques et familières des formations detritiques permo-triassiques du couloir d'Argana, Haut Atlas occidental (Maroc). Notes du Serv. Geol. du Maroc. 33 (249), 147–177.
Tourani, A., Lund, J.J., Benaouiss, N., Gaupp, R., 1999. Stratigraphy of Triassic syn-rift deposition in Western Morocco. Zentralblatt für Geologie und Paläontologie, Teil 1 Heft 9–10, 1193–1215.
Tourani, A., Benaouiss, N., Gand, G., Bourquin, S., Jalil, N.-E., Broutin, J., Battail, B., Germain, D., Khaldoune, F., Sebban, S., Steyer, J.-S., Vacant, R., 2010. Evidence of an early Triassic age (Olenekian) in Argana Basin (High Atlas, Morocco) based on new chirotherioid traces. C.R.Palevol (2010) 1–8.
Turnbridge, I.P., 1981. Sandy high-energy flood sedimentation – some criteria for recognition, with an example from the Devonian of SW England. Sediment. Geol. 28, 79–96.
Turner, P., Sherif, H., 2007. A giant Late Triassic-early Jurassic evaporitic basin on the Saharan platform, North Africa. In: Schreiber, B.C., Lugli, S., Babel, M. (Eds.), Evaporites through Space and Time. Geological Society, London, Special Publications, 285, pp. 87–105.
Turner, P., Pilling, D., Walker, D., Exton, J., Binnie, J., Sabaou, N., 2001. Sequence stratigraphy and sedimentology of the late Triassic TAGI (Blocks 401/402, Berkine Basin, Algeria). Mar. Petrol. Geol. 18, 959–981.
Van Houten, F.B., 1977. Triassic-Jurassic deposits of Morocco and E North America: comparison. AAPG Bull. 61 (1), 79–99.
Veevers, J.J., 1994. Pangaea: evolution of the super-continent and its consequences for earth's palaeoclimate and sedimentary environments. In: Klein, G.D. (Ed.), Pangaea: Palaeoclimate, Tectonics and Sedimentation during Zenith and Break-up of a Super-continent, Geological Society of America Spec. Pub., 288.
Verati, C., Rapaille, C., Féraud, G., Marzoli, A., Bertrand, H., Youbi, N., 2007. $^{40}Ar/^{39}Ar$ ages and duration of the Central Atlantic magmatic province volcanism in Morocco and Portugal and its relation to the Triassic–Jurassic boundary. Palaeogeogr. Palaeoclimatol. Palaeoecol. 244 (1–4), 308–325.
Voigt, S., Hminna, A., Saber, H., Schneider, J.W., Klein, H., 2010. Tetrapod footprints from the uppermost level of the Permian Ikakern Formation (Argana Basin, Western High Atlas, Morocco). J. Afr. Earth Sci. 57, 470–478.
Wang, P.X., 2009. Global monsoon in a geological perspective. Chin. Sci. Bull. 54, 1113–1136.
Whiteside, J.H., Olsen, P.E., Eglinton, T., Brookfield, M.E., Sambrotto, R.N., 2010. Compound-specific carbon isotopes from Earth's largest flood basalt eruptions directly linked to the end-Triassic mass extinction. Proc. Natl. Sci. U. S. A. 107, 6721–6725.
Wills, L.J., 1970. The Triassic successions in the Central Midlands in its regional setting. Q. J. Geol. Soc. Lond. 126, 225–283.
Wright, V.P., 1992. Paleopedology: stratigraphic relationships and empirical models. In: Martini, I.P., Chesworth, W. (Eds.), Weathering, Soils and Paleosols. Elsevier, Amsterdam, pp. 475–499.
Wright, V.P., Mariott, S.B., 1993. The sequence stratigraphy of fluvial depositional systems: the role of floodplain sediment storage. Sediment. Geol. 86, 203–210.
Wright, V.P., Marriot, S.B., 1996. A quantitative approach to soil occurrence in alluvial deposits and its application to Old Red Sandstone of Britain. Q. J. Geol. Soc. Lond. 153, 907–913.
Youbi, N., Martins, L.T., Munha, J.M., Ibouh, H., Madeira, J., Ait Chayeb, El Boukhari, A., 2003. The Late Triassic-early Jurassic Volcanism of Morocco and Portugal in the framework of the Central Atlantic magmatic province: an overview. In: Hames, W.E., McHone, J.G., Ruppel, C. (Eds.), The Central Atlantic Province: Insights from Fragments of Pangea, AGU, Geophys. Mon, 136, pp. 179–207.
Young, J.A., 1987. Physics of monsoons: the current view. In: Fein, J.S. a. S. (Ed.), Monsoons. Wiley, New York, pp. 211–243.